BUCKLING ANALYSIS OF SINGLY CURVED SHALLOW BI-LAYERED ARCH UNDER CONCENTRATED LOADING

A Thesis

by

MAHESH SONAWANE

Submitted to the Office of Graduate Studies of
Texas A&M University
in partial fulfillment of the requirements for the degree of

MASTER OF SCIENCE

August 2007

Major Subject: Mechanical Engineering

BUCKLING ANALYSIS OF SINGLY CURVED SHALLOW BI-LAYERED ARCH UNDER CONCENTRATED LOADING

A Thesis

by

MAHESH SONAWANE

Submitted to the Office of Graduate Studies of
Texas A&M University
in partial fulfillment of the requirements for the degree of

MASTER OF SCIENCE

Approved by:

Chair of Committee, Jyhwen Wang
Committee Members, Steve Suh
Robert Bolton
Head of Department, Dennis O'Neal

August 2007

Major Subject: Mechanical Engineering

ABSTRACT

Buckling Analysis of Singly Curved Shallow Bi-layered Arch under Concentrated Loading. (August 2007)

Mahesh Sonawane, B.E., Government College of Engineering, Pune

Chair of Advisory Committee: Dr. Jyhwen Wang

Bi-layered materials are a reduced weight derivative of the sandwich structure and are comprised of one thin skin face reinforced by a thick layer of low density material. Bi-layered materials are characterized by high flexural stiffness and are a viable alternative to conventional sandwich materials in applications where the functional requirements can be met without the second face sheet of the sandwich. For structural applications bi-layered materials are required to have oil canning and buckling resistance. This work addresses the buckling of shallow bi-layered arches using numerical and analytical approaches. A numerical, finite element model is developed to simulate the buckling phenomenon and the results were compared with known experimental data. An analytical model was developed using the energy method analysis and the buckling load was predicted from the minimum energy criterion.

Comparison of the numerical and analytical results yielded fairly good agreement. An imperfection analysis conducted by means of the numerical model indicated that the load carrying capacity of bi-layered structures is reduced by up to 40% due to the presence of

material and geometric imperfections. A parametric study conducted using the analytical model has been described to setup design guidelines for shallow bi-layered arches. It was found that the use of bi-layered structures can result in weight reduction of around 70% when compared with equivalent single layered structure.

DEDICATION

I would like to dedicate this thesis to my parents who have been a huge influence in my life and wholeheartedly supported me in all my endeavors. I would also like to dedicate the thesis to my sister, who has been a constant source of encouragement and one of my best friends.

ACKNOWLEDGEMENTS

I would like to express my gratitude towards my advisor Dr. Jyhwen Wang with whose guidance, support and inspiration this thesis work has been possible. I highly appreciate his efforts to challenge my knowledge and technique to achieve nothing but excellence.

I would also like to thank Dr. Steve Suh and Dr. Robert Bolton, my thesis committee members. Their comments, suggestions and co-operation played a huge part in successful completion of this work.

I would like to thank Dr. Ke Li for his guidance and advice on various matters. I would also like to thank fellow students Shuan Huang, Liang Zhang, Monish Mamadapur and Dhananjay Salunkhe for their input and valuable suggestions on the work.

NOMENCLATURE

c	Foam thickness
f	Width of arch
r	Radial distance between any point in the section and the neutral axis, $R - R_s$
t	Face sheet thickness
u, v, w	Displacements in the axial, tangential and radial directions respectively
w_b	Displacements due to bending
w_s	Displacements due to shear
E	Modulus of elasticity of face sheet
G	Modulus of rigidity of core
H	Total energy
L_{eff}	Effective length of column
P	Concentrated load at the center of the arch
R	Radius of the neutral axis
R_s	Radius at any point in cross section
S	Span of the arch
U	Strain energy
U_b	Strain energy due to local bending strain in face sheet
U_m	Strain energy due to membrane strain in face sheet
U_s	Strain energy due to shear strain in the foam,

V	Potential energy
Vc	Volume of the core
Vf	Volume of the face sheet
β	Included angle of the arch
ε_b	Local bending strain in the face sheet
ε_{rr}	Normal strains in the radial direction in the face sheet
ε_{ss}	Membrane strains in the face sheet
γ_{ra}	Shear strains in the ra plane
γ_{rs}	Shear strains in the rs plane
γ_{sa}	Shear strains in the sa plane
λ	Shear co-efficient which is a measure of strain
θ	Angle up to any given section
χ	Geometrical arch parameter, $\chi = \beta^2 R / t$

TABLE OF CONTENTS

Page

Page

Page

LIST OF FIGURES

Page

Page

Page

LIST OF TABLES

Page

1. INTRODUCTION

Modern industries are constantly facing the new challenges of conserving the natural resources. This calls for innovation in different aspects of the design process. Innovative designs such as use of modern light weight composite materials are the need of the hour and such concepts are fast replacing the conventional materials in different fields. (Purdue webpage, 2007)

1.1 Sandwich structures

One of the technological developments of the last century is the sandwich structure. A *sandwich structure* can be defined as a structure comprised of two thin skin faces separated by a thick layer or core of low density material (Allen, 1969). The technology of sandwich structures and materials has developed a great deal in the recent years and the use of sandwich structures and materials in a variety of products has increased significantly. Sandwich structures represent a special form of laminated composite materials, where a relatively thick, lightweight and compliant core material separates thin stiff and strong face sheets. The faces are usually made of laminated polymeric based composite materials whereas the core is generally made from polymeric foam, honeycomb material or a corrugated sheet of metal. A structure of this kind results in a material of very high stiffness to weight ratios. Figure 1.1 shows a sandwich cross section with 2 face sheets of thickness t and a core of thickness c. (Allen, 1969)

This thesis follows the style of *International Journal of Solids and Structures.*

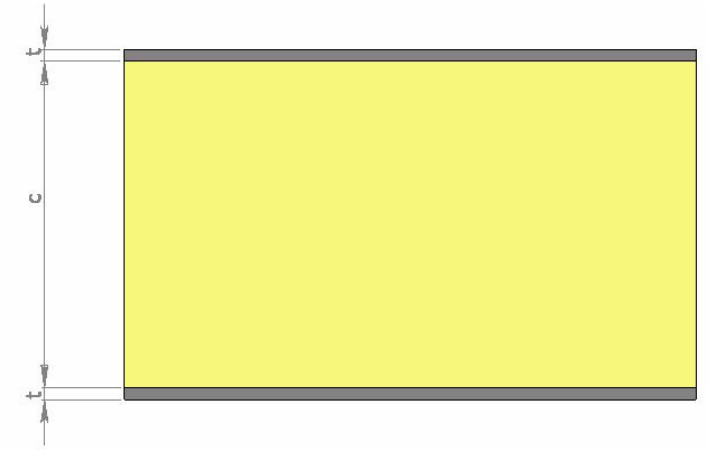

Figure 1.1: Sandwich structure

In a sandwich construction the core has several vital functions. These have been identified by Allen (1969) in his book and can be enlisted a follows:

1. The core must be stiff enough in the direction perpendicular to the faces to ensure that the faces remain the correct distance apart.
2. It must be stiff enough in shear so that the faces don't slide over each other when the panel bends. With a very weak core the sandwich will merely behave like two independent beams.
3. The core must be sufficiently stiff to hold the two face sheets flat and inhibit local buckling, also known as wrinkling, under the action of compressive stresses parallel to sandwich.

The adhesive is another important component and it should not be flexible enough to allow significant relative movement between the faces and core. The core of sandwich panel can be of different types. Aircraft structures invariably employ metal face with

honeycomb or corrugated cores (Allen, 1969). The honeycomb is a matrix formed from strips of thin aluminum alloy or steel foil. The corrugated core is a fluted metal attached alternately to the upper and lower face. Figures 1.2 –1.4 show the different types of sandwich cores.

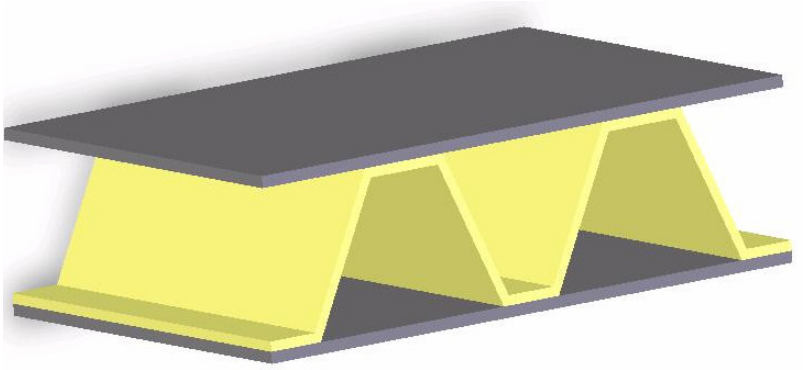

Figure 1.2: Sandwich panel with corrugated core

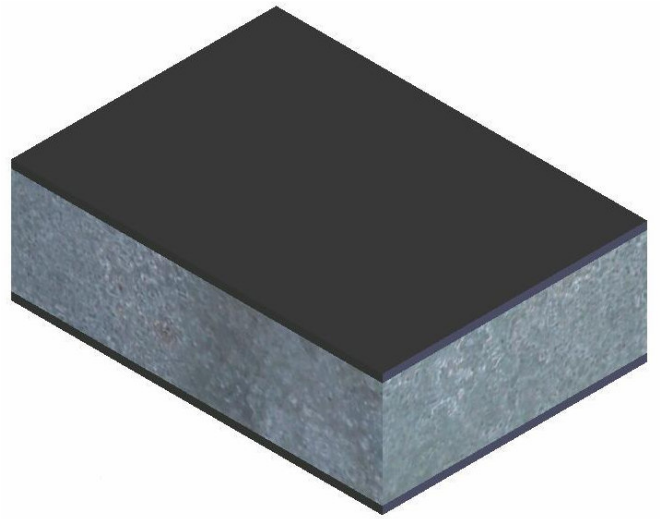

Figure 1.3: Sandwich panel with expanded plastic core

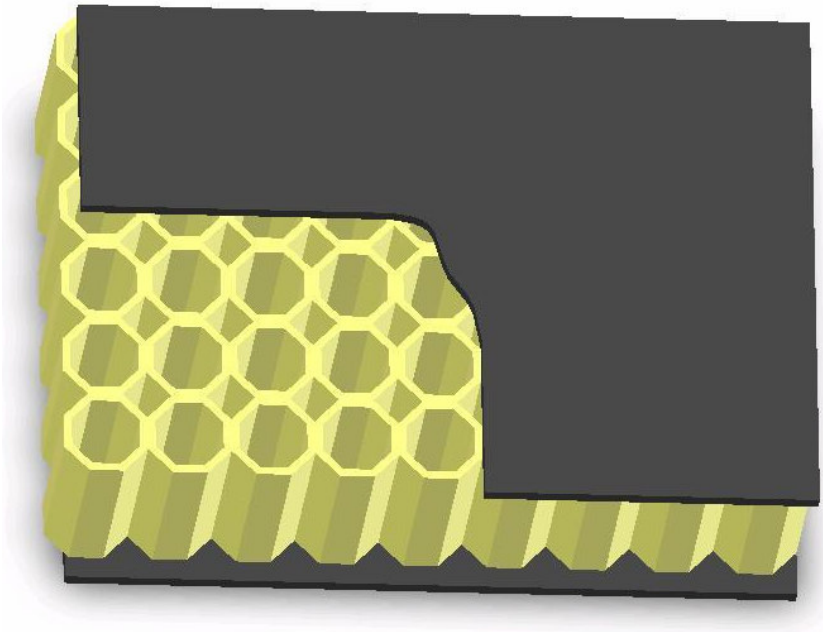

Figure 1.4: Sandwich panel with honeycomb core

1.2 Bi-layered materials

A *bi-layered structure* is a reduced weight derivative of the sandwich structure and is comprised of one thin skin face reinforced by a thick layer of low density material. Sandwich panels have been used for weight reduction in aerospace industry. Automotive body structures are different from aircraft structures and are typically manufactured by converting flat blanks into complex three dimensional shapes using sheet forming operations. Due to core failure (collapsing) in the forming operations, previous efforts in forming metal-foam-metal sandwich sheet failed to produce successful results.

A bi-layered panel manufactured using *hydro-forming* techniques can be a very viable alternative to sandwich panels. Molding of foam into a designed cavity and adhesive bonding of the molded foam onto the matching (deformed) sheet metal is a direct way of making light-weight closure panels. As flat bi-layered blanks can be produced economically, a significantly different, but low-cost, approach to produce the shaped panel is through forming of flat bi-layered blanks. Thus a bi-layered material has an advantage of manufacturability by a forming process where a sandwich material fails, in addition to its inherent structural characteristic of being lighter than a sandwich material. (Corona, 2006)

Bi-layered materials can find applications into a variety of products. It is a good alternative for designs where high stiffness is a requirement and all the functional requirements can be met without using the second skin or face sheet of a sandwich

material. One example of such applications is a car door panel or the hood which are subjected to loading from only one side i.e. the exterior. A bi-layered panel can offer significant weight reduction over an equivalent single layer panel in this application. Another example where a bi-layered panel can be employed is a refrigerator door. Here the face sheet of a bi-layered material can form the exterior surface and the foam can serve as an insulating media on the inner side in addition to strengthening the outer panel.

In real life applications all structures are subjected to a variety of loadings. Different applications have different requirements which could require high strength or high stiffness. For bi-layered structures using a thin sheet metal face the stiffness requirements are more prominent and dominate the lateral displacements of the structure. Insufficient structural stiffness can lead to two different failure phenomenons. *Column buckling* can be defined as a loss of axial capacity due to gross lateral deflection of a slender element, generated by a compressive load (Unistates Webpage, April 2007). Buckling is related to the stiffness and the slenderness ratio of the structure. An example of a structure likely to buckle is a strut under axial compressive loading as shown in Figure 1.5. (Pytel and Singer, 1987)

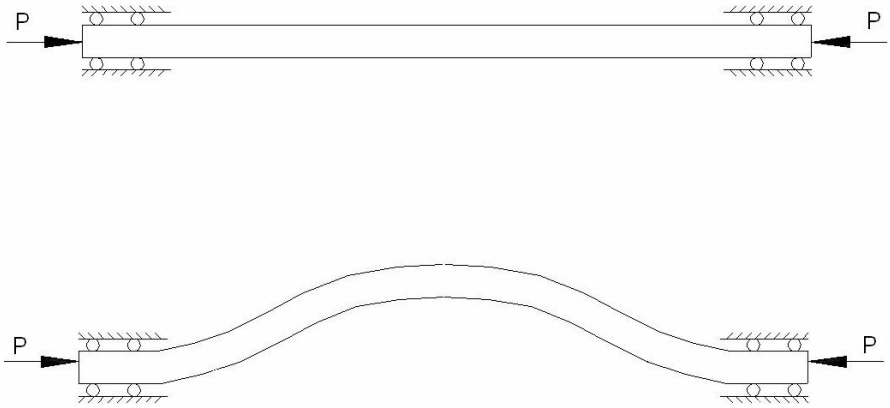

Figure 1.5: Column buckling under axial loading

Another phenomenon similar to column buckling is *Oil Canning* or *snap through buckling*. It is a moderate deformation or buckling of sheet material, particularly common with flat sheet metal surfaces. This terminology also refers to the popping sound made when pressure is applied to the deformed sheet forcing the deformation in the opposite direction**.** (U.S. Department of Transportation – FHWA, 2007). Though not a permanent deformation, oil canning deformation is a very important phenomenon in certain applications like automotive hoods and doors where the customer may perceive the temporary deflection as a poor vehicle quality or a weak design. The oil canning phenomenon is shown in Figure 1.6.

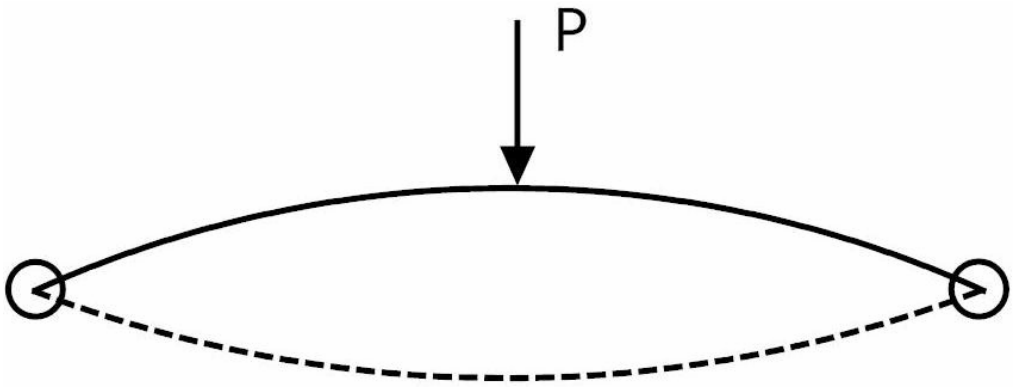

Figure 1.6: Oil canning

Buckling resistance of a panel is defined by the limiting load that a panel can carry without undergoing sudden large deflections. *Singly curved* structures are simple arches or a curved beam structures having one direction of curvature. *Shallow arches* can be defined as an arch with a small rise to span ratio. Skvortsov and Bozhevolnaya (1997) have used this criterion for classifying an arch as shallow or non-shallow by considering the h^2/S^2 ratio, if $h^2/S^2 <<< 1$ the arch can be said to be shallow. Dimensions h and S are as shown in Figure 1.7. Bradford et al. (2002) classified arches as shallow if the included angle is less than 90°. *Symmetric buckling* (Figure 1.8) for an arch is the mode of buckling in which the buckled shape remains symmetric with the plane of symmetry of the initial configuration of the arch.

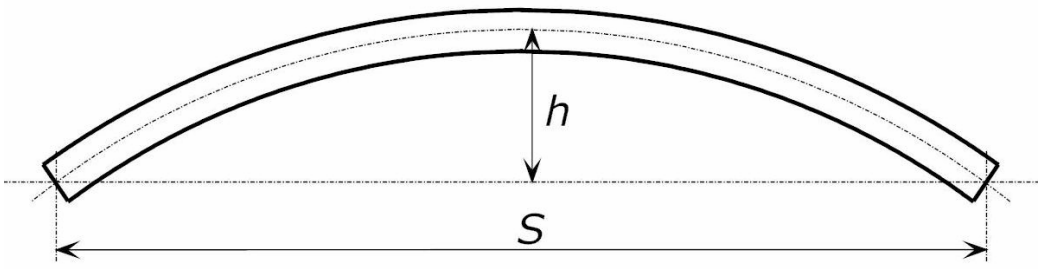

Figure 1.7: Shallow arch

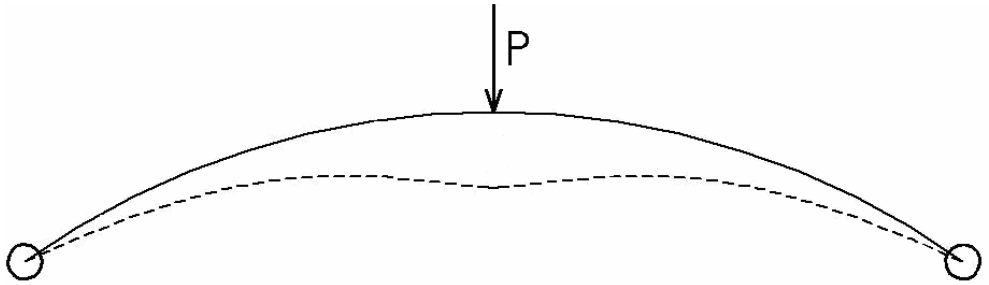

Figure 1.8: Symmetric snap through buckling mode

1.3 Research objective

Lateral buckling is one of the critical failure modes for sandwich as well as for bi-layered materials. Under a normal working life cycle a panel or general structure built using a bi-layer construction may be subjected to a variety of loading. Accurate prediction of the panel deformation and buckling limits is essential for obtaining a reliable and optimal structural design. One of the biggest challenges in using the curved

sandwich panel or a bi-layer panel is predicting the load carrying capacity of these structures.

The aim of this research is to investigate the load deformation response and estimate the limiting buckling load of the symmetric-snap through buckling mode of a singly curved shallow bi-layered arch structure under a concentrated load at the center. The configuration of the problem is schematically shown in Figure 1.9. The objective of this research is to find an approximation of the limiting buckle load and to define pre-buckling deformation. A numeric parametric study to evaluate the response of the arch under a range of geometric parameters was conducted.

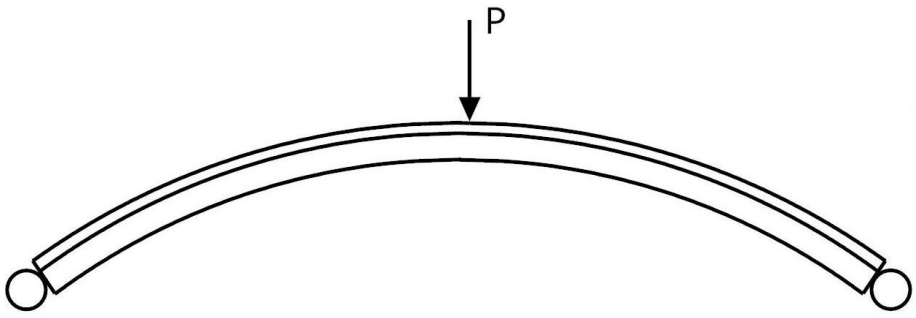

Figure 1.9: Bi-layered arch under concentrated load

1.4 Proposed work

The details of the bi-layered arch buckling problem analyzed here can be summarized as follows:

1) Structure: Singly curved bi-layered arch
2) Materials: Metal for the face sheet and foam as the reinforcing thick layer
3) Boundary conditions: Clamped or pinned on the two ends
4) Loading condition: Concentrated load at the point of symmetry

In this research, two different techniques, an analytical model and a numerical analysis are employed analyze the pre-buckling deformation and find a good approximation of the limiting buckling loads. Finite element simulation using ABAQUS software will be used for numerical analysis. Buckling analysis can be run in ABAQUS using two different methods (ABAQUS Users manual, 2007):

Eigen value analysis: ABAQUS/Standard contains a capability for estimating elastic buckling by Eigen value extraction. This estimation is typically useful for long slender structures, where the pre-buckling response is almost linear.

Riks method: This is a more powerful algorithm and predicts good results for unstable problems where during periods of the response, the load and/or the displacement may decrease as the solution evolves. It is a tool to solve geometrically nonlinear static problems involving buckling or collapse behavior, where the load-displacement response

shows a negative stiffness and the structure must release strain energy to remain in equilibrium. The problem can include non-linear material and boundary conditions.

This research work will employ the Riks method algorithm to find the buckling load. For computational efficiency the symmetry of the problem will be exploited and plane strain elements will be used to reduce the 3D model to a 2D model.

Analytical solution for a buckling problem is fairly complicated. Previous works on analytical solutions of single layered and sandwich arches have developed very complex results by solving the governing equilibrium equations. It is proposed here to develop a model that will predict the buckling load for bi-layer arch by using the energy method. Energy method is a very useful approach for complex stability analysis and it is believed that this approach should give a fair approximation to the desired result. (Gjelsvik and Bodner, 1962)

1.5 Expected contribution

Work has been done in areas of buckling of single layer arches as well as sandwich arches. This research is expected to contribute in an unexplored field of bi-layered structures. A finite element model and an approximate analytical solution for predicting the buckling load of a bi-layer arch structure will be the outcome of this work. The finite element model will be useful in mapping the displacement and stress-strain field in the bi-layered structure in addition to fulfilling the main purpose of predicting the buckling load. The analytical model will provide an understanding of this structural behavior and

relate it with various geometric parameters and material properties. The research results are expected to have broad applications in different industries.

2. LITERATURE REVIEW

Stability analysis has been the area of interest of many researchers. Large steel columns and arches or curved beams have been of special interest in this field because of their large scale use in critical engineering structures. In recent years the research in sandwich structures has gained momentum because of their increased application in different fields. Sandwich materials are known to have a high stiffness to weight ratio because of their inherent structure, however a good knowledge of their behavior under the subjected loading and boundary conditions is necessary before they can be put into practical application through an optimal design. Research in the area of sandwich columns with in plane compressive loading has made huge strides but very little has been written about curved sandwich panels or arches under lateral loading. In this section the work done in the areas of sandwich columns, plates, stability of arches along with literature pertaining to the sandwich theory and stability theory will be reviewed.

2.1 Stability theory

Timoshenko (1936) has presented extensive literature on stability of different elastic members. His book treats different stability problems like axially compressed bars, thin plates under compression, rings under compression, lateral buckling of beams, axial compression of cylindrical shells. The book treats the problem of curved bar under uniform lateral pressure, however no mention is found of the problem of a curved bar under concentrated loading. Similar work in the area of structural stability is found in Bazant (1989) and Alfutov (1999). An excellent understanding of the concept of stability

has been presented by Gregory (1967) in his book which mainly deals with the stability of framed structures. Simple illustrations like “cup and ball system” and “rod and spring system” have been presented in his work. Solutions to these stability problems have been demonstrated using the energy method and the Rayleigh method. The book covers the problem of axially loaded columns but does not treat any problem related to stability of curved beams and shells.

Another book on stability by Dym (1974) has introduced the concept of stability, stability theorems, and theorem of minimum potential energy. The von Karman theory of plates has been explained meticulously. Problems of buckling and post buckling of elastic columns, buckling of rectangular plates and circular plates have been presented in his work. Equations for shallow arches and closed form solution to the problem of stability of shallow arches are found in his work.

Modern day analytical methods like the variational principles of elasticity and the finite element method have been presented by Shames and Dym (1985). Solutions of various elasticity problems using energy method have been illustrated. They have addressed the elastic stability problems of columns and plates using the energy method. Finally, using the variational principles as a foundation they have introduced finite element solutions to some of the problems addressed in the book.

Rajasekaran and Padmanabhan (1989) in their work on curved beams have derived governing equations based on the large displacement theory for solving curved beam problems. They have used the principle of virtual work to establish the governing equations. The formulation is independent of the deformed member and thus has widespread application.

A more recent work by Gambhir (2004) in his book has addressed stability problems of key structural elements like columns, beams, rigid frames, thin plates, arches, rings and shells. The text covers basic principles of mechanics. Equations of equilibrium, fundamental principle of work and strain energy, energy theorems have been dealt with in his work. Different methods to obtain a solution like the trial function method, Galerkin method, finite difference method and numerical integration are illustrated with simple examples. The book does not consider any problem involving sandwich structures. The problem of a singly curved arch loaded with a uniform pressure on the lateral surface is covered.

2.2 Sandwich theory

Detailed work in the area of theoretical analysis of sandwich beams, plates and struts has been done by Plantema (1966), Allen (1969) and Zenkert (1995). Plantema (1966) has covered different problems of bending and buckling of sandwich struts, columns and plates under in-plane loading. Beam theory applicable to sandwich structures has been presented in his work. Buckling problems of sandwich columns, plates under axial compressive loading have been solved using the energy method. Theory of sandwich

panels has been presented meticulously followed by various design formulas pertaining to the design of sandwich beams and struts. Allen (1969) and Zenkert (1995) have presented similar work in the area of sandwich panels. Design guidelines for sandwich beams and columns, beam theory for a sandwich structure and the governing equilibrium equations are found in their work.

Using the theory from Allen (1969), Heder (1991) has compared the buckling load of sandwich panel obtained by analytical method and finite element analysis. Approximate buckling loads for panels with different boundary conditions have been derived using an energy method analysis. Different combinations of end conditions like simply supported edges and clamped edges are used while the panel is under axial compression loading. Buckling coefficients and buckling loads were derived for four different boundary conditions.

More thorough work on sandwich panel buckling has been done by Mahfuz, Islam, Saha, Carlsson and Shaikh (2005) in their analytical, experimental and finite element study to investigate the effect of core density and core sheet de-bonding on buckling of sandwich panel. The configuration considered was a sandwich column loaded axially and having pinned ends. The experimental work involved tests conducted with various foam densities and also with implanted de-lamination between the core and the face sheet. The intent was to investigate the effect of core density, and the effect of core–skin de bonds on the overall buckling behavior of the sandwich. Analytical and finite element

calculations were also performed to support the experimental observations. They observed that core density has direct influence on the global buckling of the sandwich panel, while embedded de-lamination seem to have minimal effect on both global as well as local buckling. The analytical calculations considered a modification to the Euler's load to take into account the shear deformation of the core.

2.3 Research in arch buckling

Langhaar, Boresi and Carver (1954) have presented an analysis of buckling of single layered circular rings and arches based on energy theory of buckling. The hoop strain formula, which is expressed in terms of the displacement of the centroidal axis, was used for deriving the strain energy equation. They solved the problem of a semicircular arch loaded by a concentrated load at its center. Experiments were conducted by using aluminum alloy strip arches and loading them in small increments with dead weight until buckling occurred. The experimental loads were in good agreement with the results obtained from their analysis.

A method to study the nonlinear buckling of single layered shallow cylindrical shells was presented by Stack-Taikidis (1972). Their study is concerned with the buckling of a thin shallow cylindrical shell under uniform lateral pressure, with boundaries fixed along the generatrix and simply supported along the directrix. The general nonlinear theory with respect to strains and the Kirchoff-Love approximations as applied to shallow shells were used for the mathematical formulation of the problem. The governing equations are expressed in terms of a stress function and the normal displacement. They have used the

Kantorovitch method to transform the nonlinear partial differential equations to a system of ordinary differential equations. A finite difference scheme was applied to transform the latter system to a system of matrix equations. An incremental technique was used to linearize the system using a computer program written in Fortran IV. The solution determines the variation of a dimensionless deflection parameter with respect to a pressure parameter. The study is valid for a single layer arch and there is no verification of results by using an alternative method.

Significant contribution to the field of analytical modeling of arch stability has been made by Gjelsvik and Bodner (1962). They have presented a critical analysis demonstrating the significance of energy criteria for snap through buckling. A rigorous experimental and theoretical analysis of single layered shallow arch buckling is presented in their work. They have investigated a simple mechanical model of two hinged bars supported by a spring to explain the concept of snap buckling. Concepts of upper bound and lower bound loads have been explained using this model. Analysis of a clamped circular arch under concentrated load is presented using the energy criteria. They carried out experiments on elastic snap through buckling of clamped arches. The objective of the experimental study was to obtain the complete load deflection curves for different geometries and the unstable regions in these curves. Comparison of the results from the two techniques showed a good agreement between the experimental load and the lower bound of the energy load.

Schreyer and Masur (1966) have taken forward the work done by Gjelsvik and Bodner (1962) and studied the buckling of single layered shallow arches. They found the exact solutions of the non-linear equilibrium equations for the clamped circular shallow arches with a detailed analysis of various buckling criteria. They have concentrated their efforts on the problem of the arch subjected to uniform pressure. The load deflection curve is obtained and they showed that for this problem both symmetric and asymmetric buckling criteria may govern. The validity of results in either case depends on the steepness of the arch. They have also dealt with the problem of a shallow arch loaded with a central concentrated load but the problem is not thoroughly analyzed and they cite the work of Gjelsvik and Bodner (1962) in that area. For the problem of concentrated load it is shown that a symmetric buckling criterion governs the problem for all degrees of steepness.

The effect of the linearization of the pre-buckling state on the determined instability loads has been analyzed by Kerr and Soifer (1969). They studied this effect on an elastic system with two degrees of freedom and on single layered shallow arch loaded with lateral uniformly distributed load. They compared the instability loads firstly obtained by an exact solution of a non-linear formulation and secondly by perturbation analysis using the linear pre-buckled state. It has been stated that for problems involving non-trivial state of stress in the pre-buckled state the linearized formulation must be used with caution because the instability may take place after the system has deformed

considerably. The problems in this category involve buckling of symmetric arches under a concentrated load at the vertex, rings and shells under non-uniform lateral pressure.

Dickie and Broughton (1971) have studied the symmetric and unsymmetrical single layered arches subjected to radial loading. They have used the energy method analysis developed by Gjelsvik and Bodner and applied the methodology to a various boundary conditions and loading conditions. Concentrated loading, uniformly distributed loading and non-uniformly distributed radial loading have been considered in their analysis. They also carried out experiments using a dead weight apparatus. Loads were applied until the arch snapped due to buckling and the radial deflections recorded at various points. The experimental and analytical results showed good agreement.

The problem of buckling and post buckling behavior of single layered shallow arches, pinned and clamped, and subject to uniform pressure was analyzed by Dym (1973). The main objective of the study was asymmetric bifurcation. Thus even though the study is concerned with shallow arches, the arches considered are steep enough so that bifurcation occurred prior to symmetric snap through. Important results from this study are that a) asymmetric bifurcation pressures have been determined by an Eigen value analysis based on a linear pre-buckling state b) such bifurcations, when the arch is steep enough so that the they occur prior to symmetric buckling, are always unstable.

Knight and Carron (1997) studied the structural response of several elastic single layered circular arches with asymmetric and symmetric boundary conditions. The effect of the arch end conditions and the subtending angle on the elastic collapse behavior was determined and described. Fixed and clamped end conditions with point load at the symmetry of the arch were considered in the study. The arch geometry considered was up to a subtended angle of 210 degrees. They briefly described a formulation for an assumed-stress hybrid beam element that exploits the co-rotational approach for solving large deflection problems. The study is mainly valid for non-shallow arches and the response, from the onset of loading, exhibited a nonlinear behavior.

Dealing with contemporary shape memory alloys (SMA) Hyo Jik Lee and Jung Ju Lee (2000) performed numerical analyses on the buckling and post-buckling behavior of laminated composite shells with embedded SMA wires. These analyses using an ABAQUS code were conducted to investigate the effect of embedded SMA wires on the characteristics of buckling and post-buckling caused by external and thermal loads. The end conditions were simply supported and clamped.

Bradford, Uy and Pi (2002) investigated analytically in-plane elastic stability of single layered arches with a symmetric cross section and subjected to a central concentrated load. They have proposed a criterion that demarcates shallow and non-shallow arches. The analysis uses a virtual work formulation to establish both - the non-linear equilibrium conditions and the buckling equilibrium equations for shallow arches.

Analytical solutions for anti-symmetric bifurcation buckling and symmetric snap-through buckling loads of shallow arches subjected to this loading were obtained. Approximations for the symmetric buckling load of shallow arches and non-shallow fixed arch and for the anti-symmetric buckling load of non-shallow pin-ended arches were obtained.

2.4 Sandwich arches

Load-deformation behavior and global stability of shallow singly curved sandwich panels subjected to lateral loading was studied by Skvortsov and Bozhevolnaya (1997). They performed a stability analysis for a simply-supported sandwich panel of constant curvature and loaded by uniform pressure. A model for the load-deformation response of a shallow singly-curved sandwich panel is developed on the basis of Reissner plate theory. For arbitrary initial panel geometry and lateral load distribution, the load deflection relations are derived in the form of two implicit equations. Explicit equations describing the deformation behavior of symmetric sandwich panels subjected to symmetric loading are also presented. The boundary conditions on both the ends in simply supported. Structural and buckling parameters which depend on the panel geometry and material properties were introduced. These parameters allow the buckling behavior of shallow sandwich panels to be predicted. The ideas behind the analysis and the solution technique are illustrated by a numerical example. The critical pressure is derived in terms of the structural buckling parameters and hence a direct relation between the geometry and this load is not found. The analysis is valid for a sandwich structure and there is no applicability of the results to a bi-layered structure.

Skvortsov and Bozhevolnaya (2001) further extended the work done by Skvortsov and Bozhevolnaya (1997) by studying the global behavior of a curved panel of arbitrary initial profile and general boundary conditions under any kind of distributed loading that can be described in terms of an infinite series expansion. Shallow singly curved sandwich panel with lateral loading is considered in the analysis. General boundary conditions are considered, i.e. boundary conditions simply supported and clamped are considered on all four edges of the arch. These represent more realistic conditions encountered in practical applications. Governing equations based on Timoshenko-Reissner plate theory are derived for these boundary conditions. Numerical analysis is carried out and the load deflection response is plotted.

In the area of finite element modeling Rose, Moore, Knight, Jr., Rankin (2002) did a comparative study of various modeling approaches for predicting the buckling behavior of sandwich panels using a sandwich panel with anisotropic faces and thick core. They used the STAGS non-linear finite element code for their numerical simulations. The results from various approaches of modeling were compared with the conventional analytical solutions for the overall buckling mode as well as the load buckling modes such as wrinkling. They concluded that the specialty sandwich element formulation as implemented in STAGS is a very effective and accurate modeling approach for predicting the sandwich behavior.

Bull and Hallstrom (2004) studied curved sandwich beams subjected to opening bending moment. They introduced face–core debonds of varying sizes at the compressively loaded face sheet and investigated the structural integrity. Analytical and finite element models are compared in order to identify the governing failure modes of the beams. A simple expression is presented as a tool for getting a quick estimate of the severity of an interface crack in a curved sandwich beam. Five different configurations of beams were tested experimentally in a custom made bending rig. They also mention that the failure mode for a curved beam as the radii increases is governed more and more by the regular straight beam theory.

In a rigorous finite element analysis of sandwich beams Lyckegaard and Ole (2006) studied the buckling behavior of a straight sandwich beam joined with a curved sandwich beam. They have created two models, one using a finite element model and other using a higher order sandwich theory. The structure was loaded on the straight beam section and the behavior of the panel in pure bending condition was investigated. The finite element model was created using ANSYS. Beam elements were used to model the sandwich faces whereas the core was modeled using the 2D solid elements. The results from the two models did not compare well necessitating some more research in this area.

2.5 Summary

The main objective of the work done in the field of stability analysis, described above, has been the study of the load deflection response of the structure. Some of them deal

with predicting the deformed shape of these structures under a given set of loading and boundary conditions. The major work done in the areas of stability analysis of sandwich structures and arches, described above has been broadly summarized in Table 2.1.

Table 2-1 Summary of the literature review

Structure	Loading Conditions	Technique
Single Layer Arches	Uniform lateral pressure / Concentrated load	Experimental / Analytical
Sandwich Plates / Columns	Axial Compression	Experimental / Analytical
Sandwich Arches	Uniform lateral pressure	Analytical / Numerical
Bi-layered Arches	Proposed research	

3. NUMERICAL MODEL

Finite element analysis is a computer simulation technique used in engineering analysis. This research will make use of the ABAQUS finite element analysis package for the stability analysis of the bi-layered arch structure. Two different methodologies exist for the buckling and post buckling problems 1) Eigenvalue prediction 2) Riks algorithm:

1) Eigenvalue buckling prediction

ABAQUS/Standard contains a capability for estimating elastic buckling by eigenvalue extraction. This estimation is typically useful for stiff structures, where the pre-buckling response is almost linear. The buckling load estimate is obtained as a multiplier of the pattern of perturbation loads, which are added to a set of base state loads. The base state of the structure may have resulted from any type of response history, including nonlinear effects. It represents the initial state to which the perturbation loads are added. The response to the perturbation loads must be linear up to the estimated buckling load values for the eigenvalue estimates to be reasonable. (ABAQUS Theory Manual, 2007)

2) Modified Riks algorithm

It is often necessary to obtain nonlinear static equilibrium solutions for unstable problems, where the load-displacement response can exhibit the type of behavior as shown in Figure 3.1 that is, during periods of the response, the load and/or the

displacement may decrease as the solution evolves. The modified Riks method is an algorithm that allows effective solution of such cases.

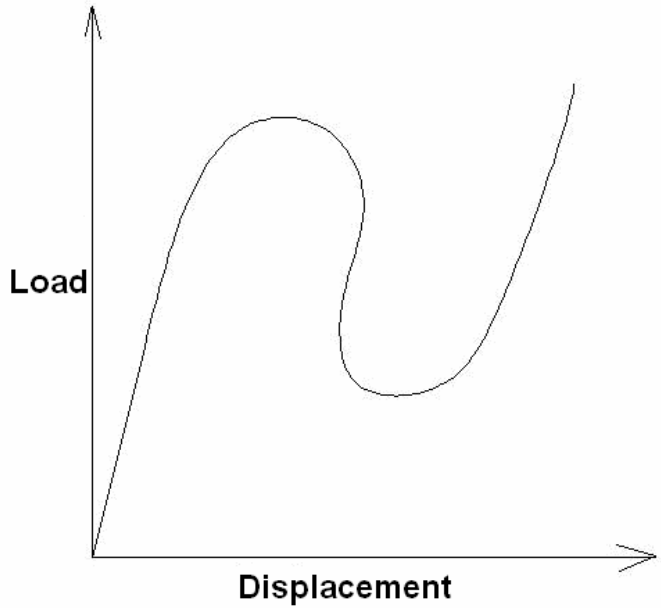

Figure 3.1: Typical unstable static response

In this algorithm, it is assumed that the loading is proportional that is, that all load magnitudes vary with a single scalar parameter. In addition, the response is assumed to be reasonably smooth, meaning that sudden bifurcations do not occur. The essence of the method is that the solution is viewed as the discovery of a single equilibrium path in a space defined by the nodal variables and the loading parameter. Development of the solution requires this path be traversed as far as required.

3.1 Finite element model for a single layer arch

Developing an appropriate finite element technique is of critical importance to obtain reliable results. Before embarking upon the task of building a complex model of a bi-layered arch it is advisable to develop model for a single layer arch subjected to similar loading and boundary conditions. Numerous analytical as well as experimental results are available for the problem of buckling of a single layer circular arch under a lateral concentrated load. This provides an opportunity to verify the finite element model by comparing the FEA results with the available results. Once the technique is validated similar model of a bi-layered arch can be built by incorporating a second layer, changing the geometrical parameters in the model and maintaining the established simulation parameters and syntax. Thus the objective of the study in this section is to establish different parameters of the finite element model by solving a simple problem of buckling of a single layer arch under concentrated lateral loading.

Dickie and Broughton (1971) have demonstrated the use of the strain energy model to find an exact solution as well as a series approximation to the problem of a buckling of clamped arches under uniform distributed load and a point load. They have proved the technique by comparing the results with experimental data. The solutions are found to be in close agreement with the experimental data. A part of the experiments conducted by them is simulated here. This data is being used for verification purpose. These results will be compared with those from the finite element technique by creating a model to the specification given in Table 3.1. In the Table geometric arch parameter ($\chi = \beta^2 R / t$) is a

dimensionless parameter of the arch. The details of the FEA model can be found in Appendix A.

Table 3-1 Arch properties

Geometric arch parameter $\chi = (\beta^2 R / t)$	Young's Modulus, E (N/mm^2)	β (degrees)	R (mm)	f (mm)	t (mm)
73.08	2895.79	30.00	2540.00	25.40	9.52
54.81	2895.79	30.00	2540.00	25.40	12.70

3.1a Single layer arch with fixed end conditions

The configuration of the arch after the snap is shown in Figure 3.2. This Figure is a plot of the von Mises stresses in the arch. The finite element simulation is run for both the arch geometries given in Table 3.1. Buckling load for the arches is found by measuring the normal reaction at the end. This reaction is plotted against the vertical displacement of the point of application of the load. Figure 3.2 shows the deformed configuration of the single layer arch and the von Mises stress field. This load deflection curve for the two geometries is shown in Figure 3.3 and Figure 3.4. The critical load is the first maximum since the point of application of load. The load increases until the arch snaps, following which there is a decrease in the load.

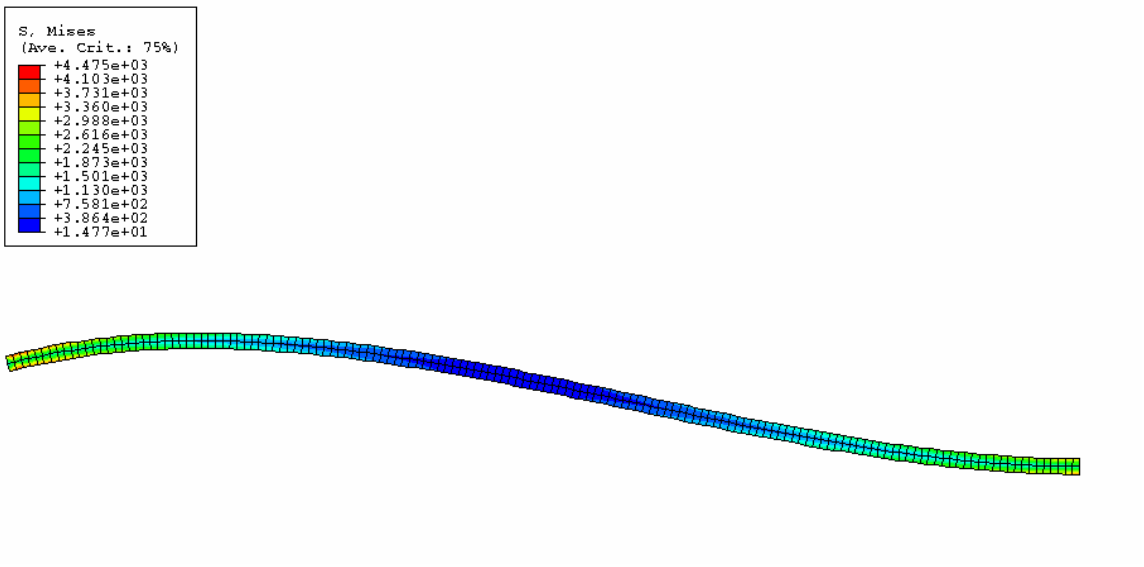

Figure 3.2: Buckled configuration of the single layer arch

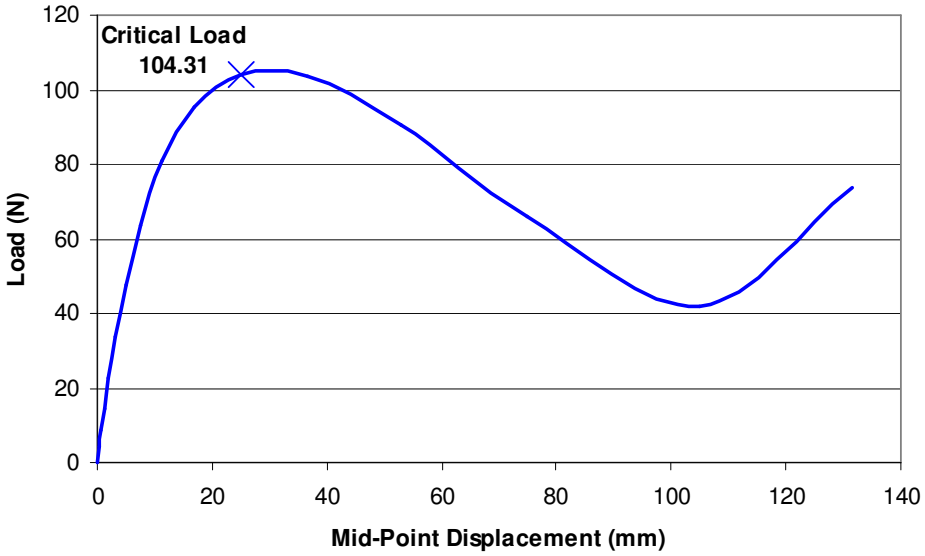

Figure 3.3: Load deflection curve of arch with 54.81 arch parameter

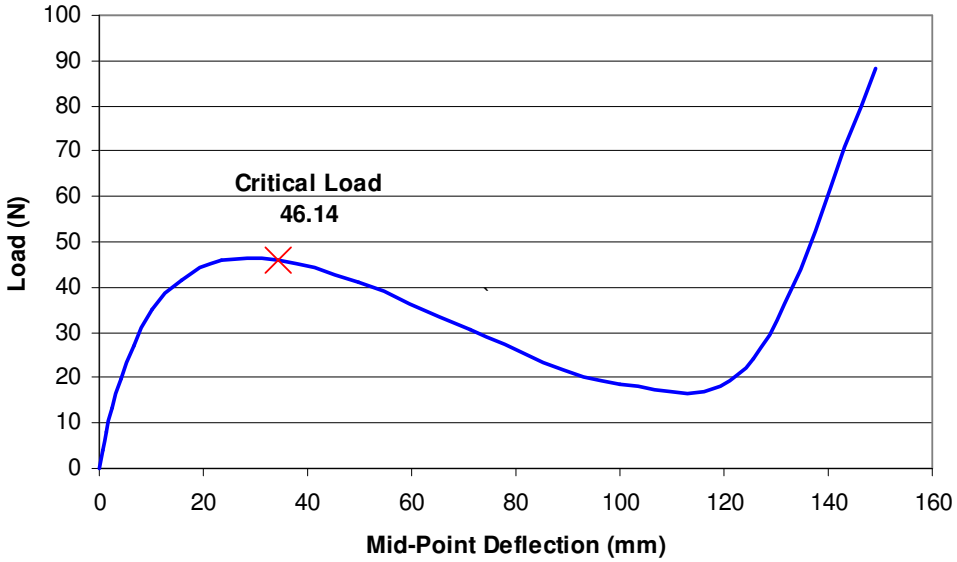

Figure 3.4: Load deflection curve for arch with 73.08 arch parameter

Table 3.2 shows the comparison of the results obtained by the three methods for the Clamped ends boundary condition. The results are in good agreement with the experimental and the analytical technique with the difference being within 5% when compared with either technique. Thus this sufficiently establishes the fact that the FEA analysis is giving reliable results.

Table 3-2 Clamped arch

Geometric arch parameter	Results from Dickie, Broughton (1971)			FEA results	Error in %	
χ	W_{series}	W_{theory}	W_{Exp}	W_{FEA}	W_{Exp} - W_{series}	W_{FEA} - W_{series}
73.08	45.91	45.02	42.82	46.13	-5.00	2.45
54.81	106.38	105.50	95.35	104.31	-10.00	-1.9

3.1b Pinned end boundary condition for single layer arch

Next task is to verify the results using the pinned ends boundary condition. Previously developed model of the single layer arch with thickness 12.70 mm was modified to impose the pin ended boundary conditions. Pinned ends boundary condition was imposed and all other parameters were kept unchanged from the previous model. The results obtained from this analysis have been illustrated below. The critical load is found by using a similar procedure as explained for the clamped arch. Figure 3.5 shows the load deflection curve of the single layer arch with pinned boundary conditions.

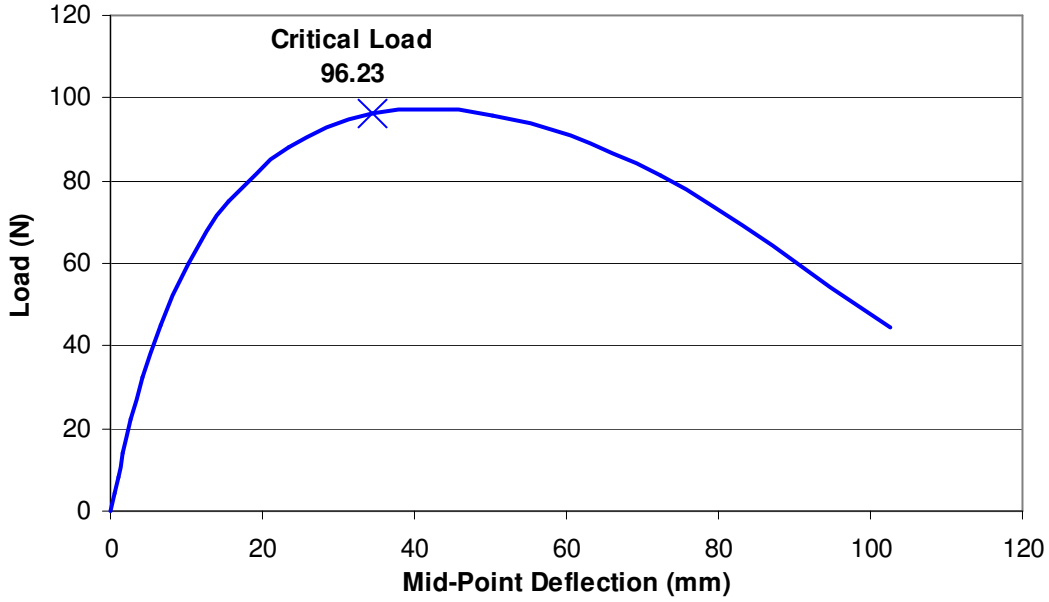

Figure 3.5: Load deflection curve for 54.81 arch parameter pinned arch

Note that the loads reported here are exact maximum values as obtained from the ABAQUS report module. The series of values obtained from different time steps are then plotted against the displacement to obtain the plots shown in Figures 3.3, 3.4, 3.5.

The results from the FEA are in good agreement with the analytically and experimentally obtained loads. From the Euler's load for a column buckling under compressive loading it is known that that the buckling load under fixed or clamped end boundary condition is greater than that in the case of a pinned end boundary condition. The results for the pinned arch shown in Table 3.3 and the clamped arch follow this trend.

Table 3-3 Pinned arch

Geometric arch parameter	Results from Dickie, Broughton (1971)			FEA results	Error in %		
χ	W_{series}	W_{Exact}	W_{Exp}	W_{FEA}	W_{Exp} - W_{Exact}	W_{series} - W_{FEA}	W_{Exact} - W_{FEA}
54.81	97.56	84.75	86.96	96.23	3	1.35	12.35

3.1c Buckling of 10 degree and 15 degree single layer arches

The single layer FEA model was further verified with experimental results from the unpublished work of Corona (2006). The arch specifications are shown in Table 3.4.

Table 3-4 Experimental specimen geometry of Corona (2006)

R (mm)	θ (°)	t (mm)
343.40	15	1.01
511.81	10	1.01

Figure 3.6 shows the load deflection curves for the experiment and the FEA for the two arches. The experimental and FEA results compared in Table 3.5 are in close agreement with the FEA prediction being higher than the experimental results. This provides sufficient confidence in the finite element model developed for the point load buckling.

Thus this model can be updated by incorporating the necessary changes to form a bi-layered arch model.

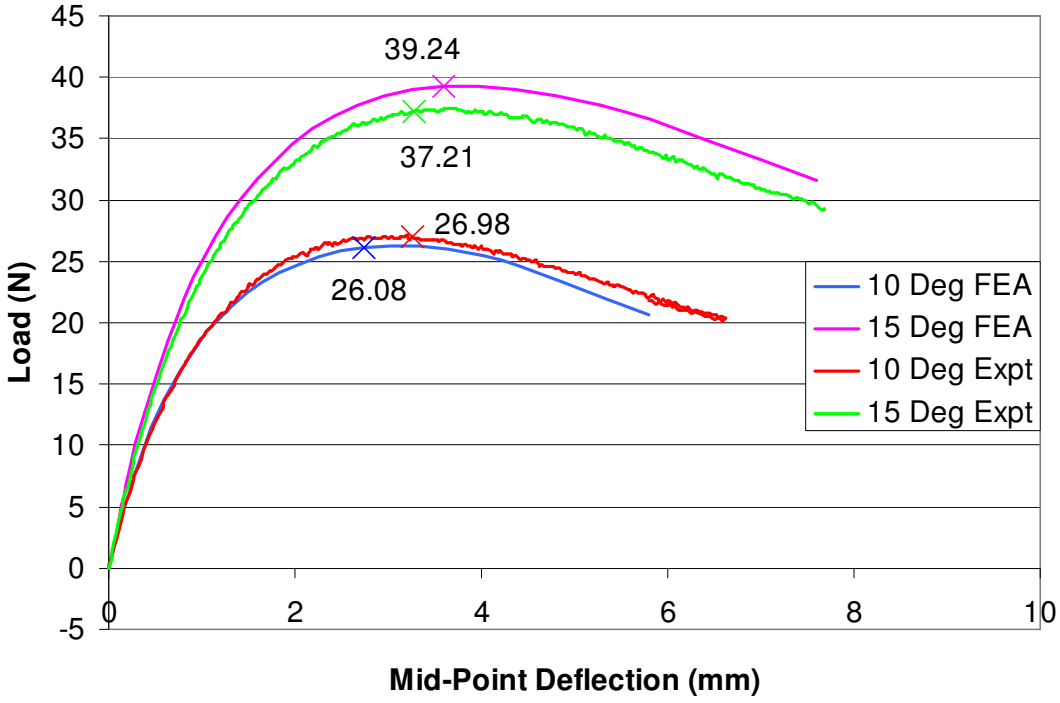

Figure 3.6: Comparison of experimental and FEA load deflection curves

Table 3-5 Comparison of single layered arch results

Configuration	FEA	Experimental	FEA-Expt
10° Arch	26.08	26.98	3.40%
15° Arch	39.24	37.21	-3.52%

3.2 Bi-layered arch experimental investigation

In this research the response of a bi-layer panel has been investigated using an analytical solution and numerical simulations using the ABAQUS FEA package. Experiments have not been conducted to measure the response. However some experimental results are available from Corona's (2006) unpublished work on buckling of a bi-layer arch. The objective of this study is to compare these experimental results with finite element simulation results for a similar model.

3.2a Experimental setup

This experimental work was done to study the influence of foam support on the stiffness and buckling of shallow arches. The specimens were shallow circular arches made of 2024-T3 aluminum sheet, with thickness of 1.01 mm (t), supported by a foam layer that was 12.70 mm (c) thick. In this study, the foam was Rohacell 71. The arches were tested in the configuration shown schematically in Figure 3.7. A special loading fixture was constructed to allow testing of arches of different depths, represented by the angle θ. The fixture was mounted on a screw-driven testing machine. The detailed experimental setup is shown in Figure 3.7.

3.2b Specimen preparation

The specimens were constructed by first cutting 12.7 mm wide strips of 2024-T3, aluminum sheet of 1.01 mm thickness. The sheets were subsequently rolled to achieve the desired curvature. The Rohacell 71 foam was then cut to the right shape and dimensions from a board using a band saw and a pattern that had been printed on paper.

Subsequently, the aluminum sheet and the foam were bonded with an epoxy adhesive using a vacuum bag method.

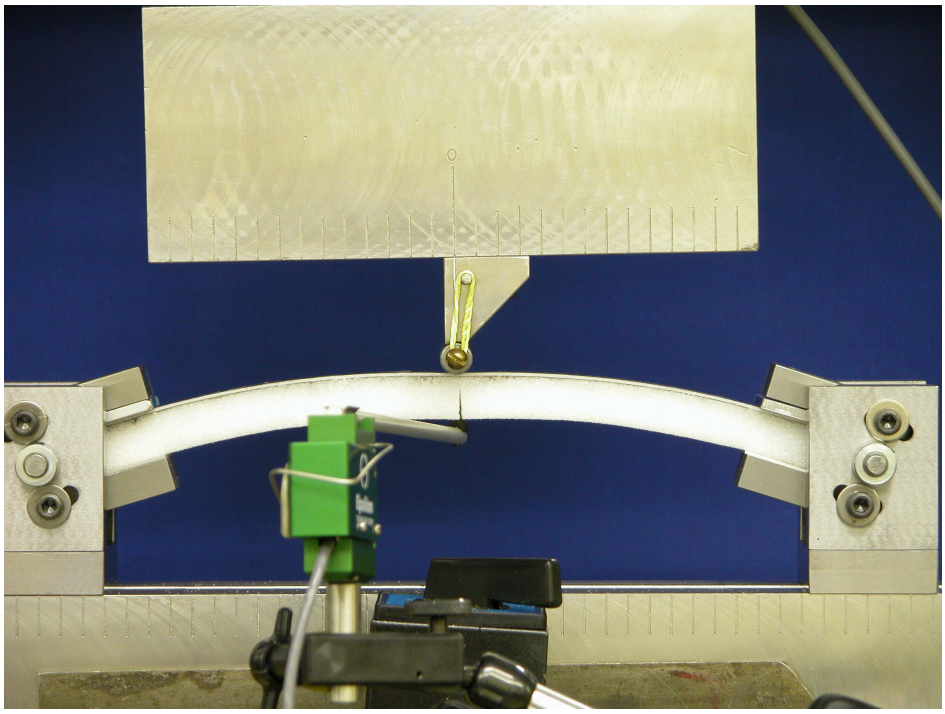

Figure 3.7: Experimental setup (Courtesy Dr. Corona)

3.2c Experimental procedure

The central point load P was applied through a steel cylinder as in Fig. 3.7. Loading was conducted in a displacement control manner until the specimens failed or the load deflection response achieved a load maximum. The load was measured using a load cell and the mid-span deflection (δ) with the same displacement transducer used in the previous testing. All specimens tested had a span S of 177.8 mm. The data available

from the experimental model was analyzed and the values of radius were deduced from the span and included angle using the following relation:

$$S = 2 \times R \sin(\beta / 2) \tag{3.1}$$

The geometrical and the material specifications of the specimens are given in Tables 3.6 and 3.7 respectively. Figure 3.6 shows the load deflection curves for the 10 degree and 15 degree bi-layered arches obtained form the experiments.

Table 3-6 Geometry of experimental specimen

R (mm)	$\beta/2$ (°)	t (mm)	c (mm)
343.40	15	1.01	12.70
511.81	10	1.01	12.70

Table 3-7 Material properties of experimental specimen

$E_{Al}(N/mm^2)$	υ_{Al}	$E_{Rh}(N/mm^2)$	υ_{Rh}
68947.57	0.3	90.32	0.35

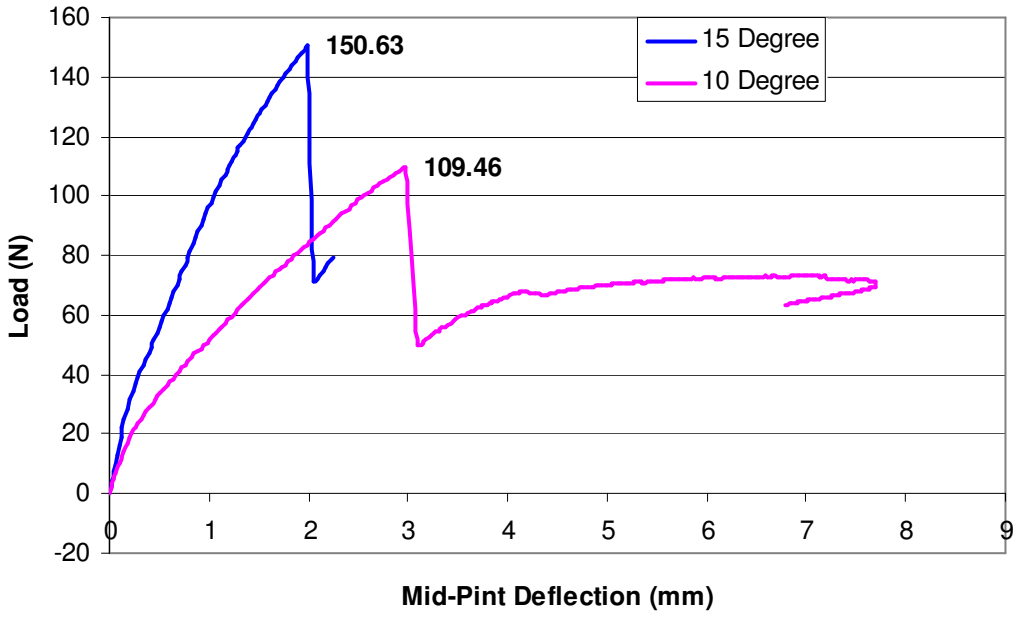

Figure 3.8: Experimental load deflection curves (Corona, 2006)

3.3 Bi-layered arch FEA model

Using the model of the single layer arch as the base the bi-layered arch was modeled by adding another layer of as the reinforcing foam. HyperMesh program was used to create the geometry of this bi-layered arch and for meshing. HyperMesh is a high-performance finite element pre and postprocessor for finite element solvers and allows for highly interactive and visual environment. The mesh generation is immensely simplified through its use and enhances the efficiency of the modeling process.

A linear isotropic model was selected for modeling the Rohacell 71 foam. Experimental data available from Corona (2006) is one of the bases of this model. Material properties

available from this experimental investigation were used while modeling the material. The buckling investigation in this research deals with the pre-buckling response of the bi-layered arch structure under quasi-static loading condition. The Elastic modulus and Poissons ratio values of 90.32 N/mm^2 and 0.35 respectively obtained from the experimental investigation were used in the analysis.

The foam was modeled using the plane strain elements CPE8 from ABAQUS. The initial simulation trials were taken by using general purpose 3D continuum elements for the foam. Subsequent trials with using the plane strain elements produced results very close to those from the 3D elements. The plane strain elements were used for all the following simulations as these are considerably computational efficient when compared to 3D elements. CPE8 elements were chosen from the plane strain element library. These are 8 node bi-quadratic elements with 9 integration points. The bi-quadratic elements are more suitable for the arch model as these can approximate the curvature more accurately. The elements of foam were grouped together in a set and the material properties of the foam were applied to this set. The interface between the foam and the face sheet was modeled to be perfectly bonded by sharing the nodes between the face sheet elements and the core elements on the interface. Rest of the parameters of the boundary conditions, loading condition and the Riks algorithm were same as the single layer model and were directly incorporated into this model. Mesh sensitivity analysis was done to select the element size or the mesh density. The details of this analysis have been presented in the Appendix B.

In the experimental investigation the bi-layered arch specimen was clamped at the ends over a length of 1 inch in the tangential direction. To facilitate proper clamping a metal layer of 1 inch length was glued on the foam on the bottom side. To represent the actual boundary conditions implemented in the experimental setup the bi-layered arch was modeled to the actual length of the specimen and clamped boundary condition was imposed on the end nodes and the nodes on the top and bottom surfaces over a length on 1 inch in the tangential direction.

3.3a Finite element simulation results

Using the geometrical and material parameters given in Tables 3.7 and 3.8 finite element models were created for the arches with 10 degrees and 15 degrees included angle. A symmetric half model was created for the 15 degree arch whereas a full model was created for the 10 degree arch in addition to its symmetric model. This full scale model was created to ensure the correctness of the symmetric models. The initial FEA model created using the experimental data predicted a higher stiffness when compared with the experimental data. However a closer examination of the experimental setup suggested the pinned boundaries to be implemented at the extreme end point of the arches which is at a larger span than given in the experimental data. Subsequent finite element simulations were conducted with due consideration to these actual boundary conditions.

The buckling load is obtained by plotting the load measured as a reaction at the clamped end against the deflection of the mid point of the arch. The load increases gradually with displacement up to a certain point and then there is a sudden decrease as the arch snaps. The first maximum is taken as the buckling load for the first mode. Figure 3.10 is a typical plot of load against the arc length obtained from ABAQUS. The arc length provides a measure of the point at which the arch snaps. This value of the arc length can be referred to when monitoring the value of stresses and strains at the point of snap. Figures 3.9 and 3.10 show the deformed shape of the 10 degree arch full model and 15 degree arch half model respectively. This image is taken at the point of snap. It maps the strain field in the arch by plotting the logarithmic strain (LE11) in the plane of the arch in direction '1'. The maximum value of the logarithmic strain LE11 at the point of snap is 0.047 for the 10 degree angle arch. The corresponding value for the 15 degree angle arch is 0.077.

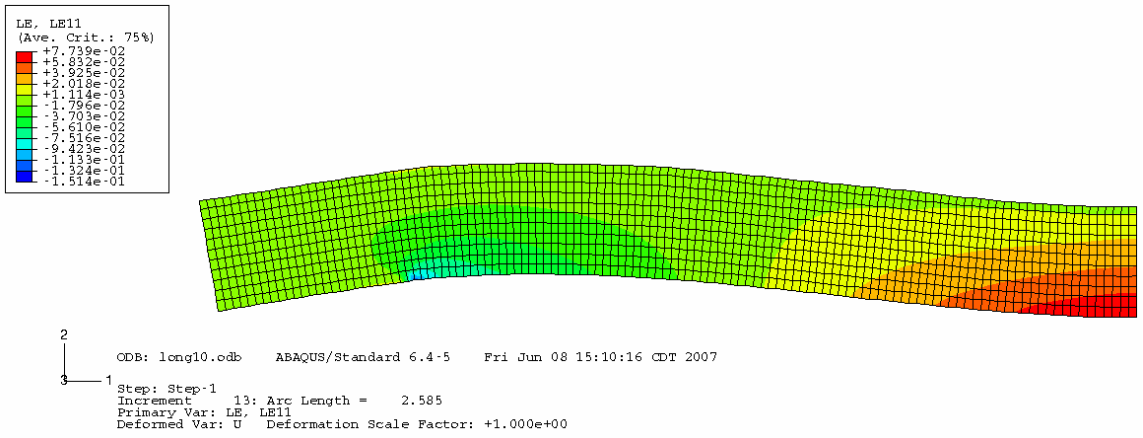

Figure 3.9: Logarithmic strain field in 10 degree arch

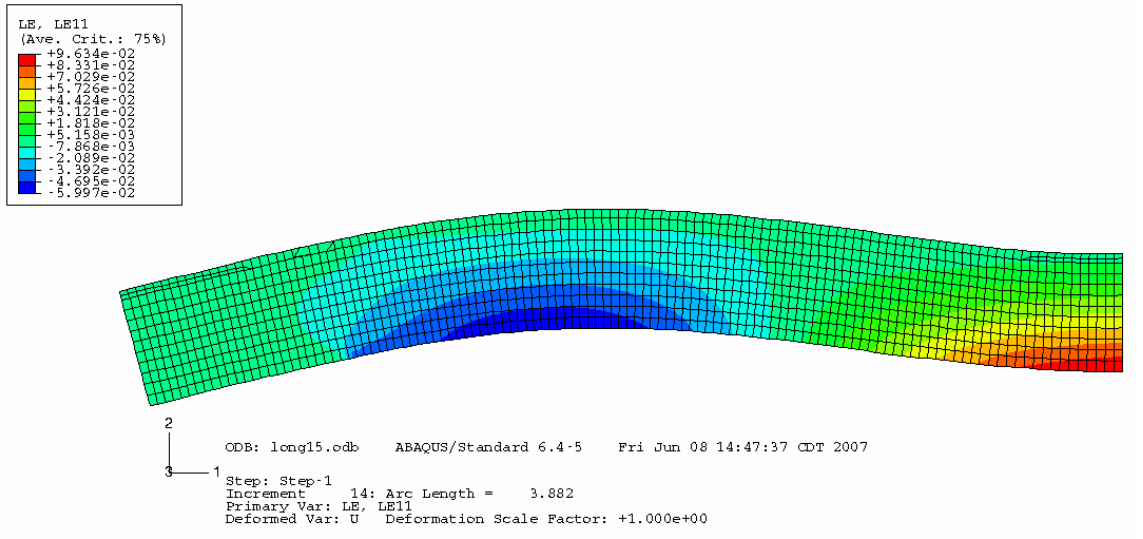

Figure 3.10: Logarithmic strain field in 15 degree bi-layered arch

Figures 3.11 and 3.12 show the load deflection curve and the critical buckling load for the two arches.

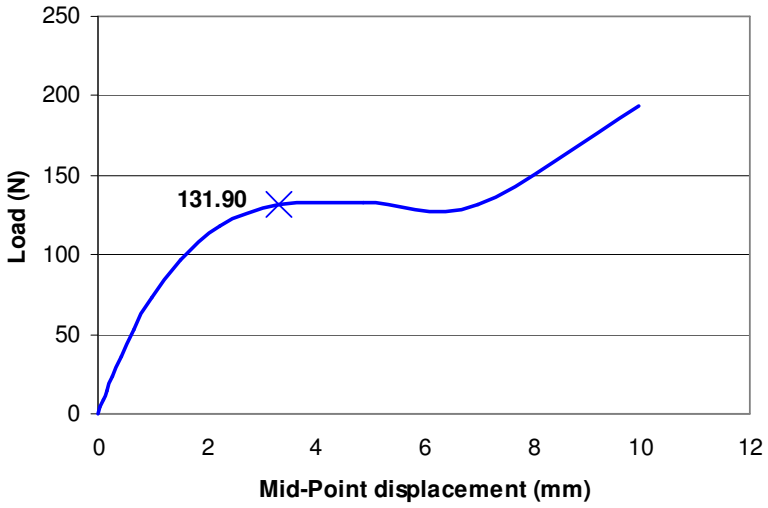

Figure 3.11: Load vs deflection for 10 degree bi-layered arch

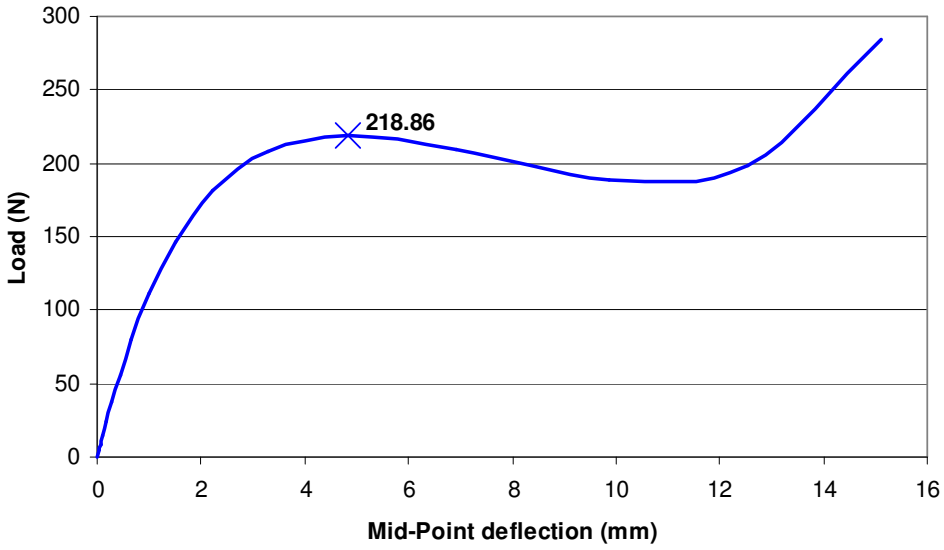

Figure 3.12: Load vs deflection for 15 degree bi-layered arch

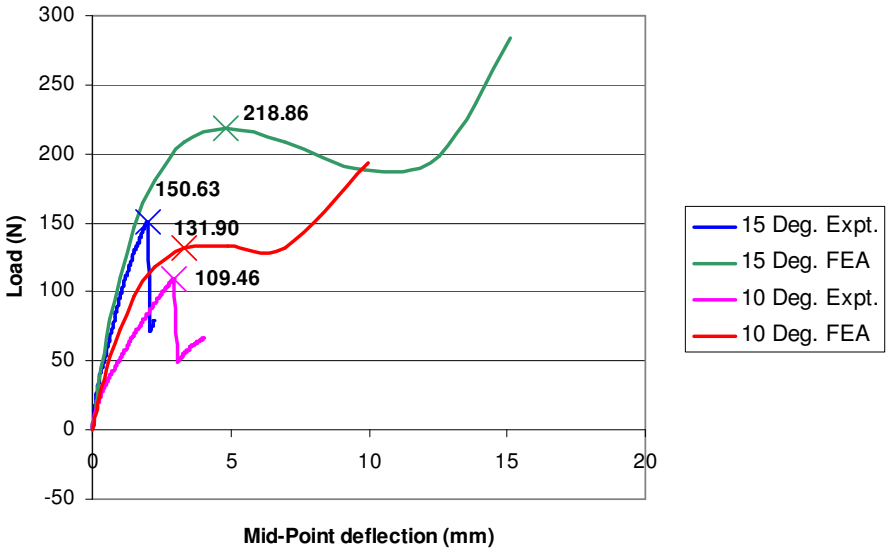

Figure 3.13: Experimental results

Figure 3.13 shows the comparison between the FEA and the experimental plots. When compared with the finite element analysis results we can see in the experimental curve that there is a sharp drop in the load from the maximum, where as in the FEA there is a gradual transition at the point of snap.

Table 3-8 Comparison of bi-layered arch buckling loads

Geometry	10 Deg Arch	15 Deg Arch
Experimental buckling load (N)	109.46	150.63
FEA buckling load (N)	131.90	218.86

3.4 Observations and discussion

The discrepancy between the analytical solution and the experimental results is often observed in stability analysis. A reason for this has been cited by Gjelsvik and Bodner (1962) from the work done by T. von Karman and Tsein. This discrepancy is said to be because of the existence of a post buckling stable equilibrium state. This state is at a load considerably lower than that predicted by classical buckling analysis. This is considered as the lowest load at which buckling is possible. The upper buckling load is the critical load at the point of snap through. The post buckling equilibrium state and the lower value of buckling load is shown in Figure 3.14. This leads to the possibility that the arch jumps to this equilibrium state at loads less than the linear buckling state. One doubt in this theory is how the transition from the initial state to buckled state took place. To support this argument Von Karman, Dunn and Tsein have suggested that the transition could be connected with the geometrical imperfections of the specimen, some dynamic disturbance or possibly with unsymmetrical deformations that are not considered in the analysis.

Dym (1973) in his analysis has shown that the unsymmetrical buckling mode is not possible for the problem of the arch loaded with a concentrated load at the center. Thus the third reasoning can be neglected however still the possibility of geometrical imperfection in the arch or a dynamic disturbance may cause the load predicted by the experimental result to be lower than that predicted by FEA. Thus the presence of a disturbance in the experimental setup can trigger the jump to the post buckling

equilibrium state without recording the snap through or the upper buckling loading in the experiment.

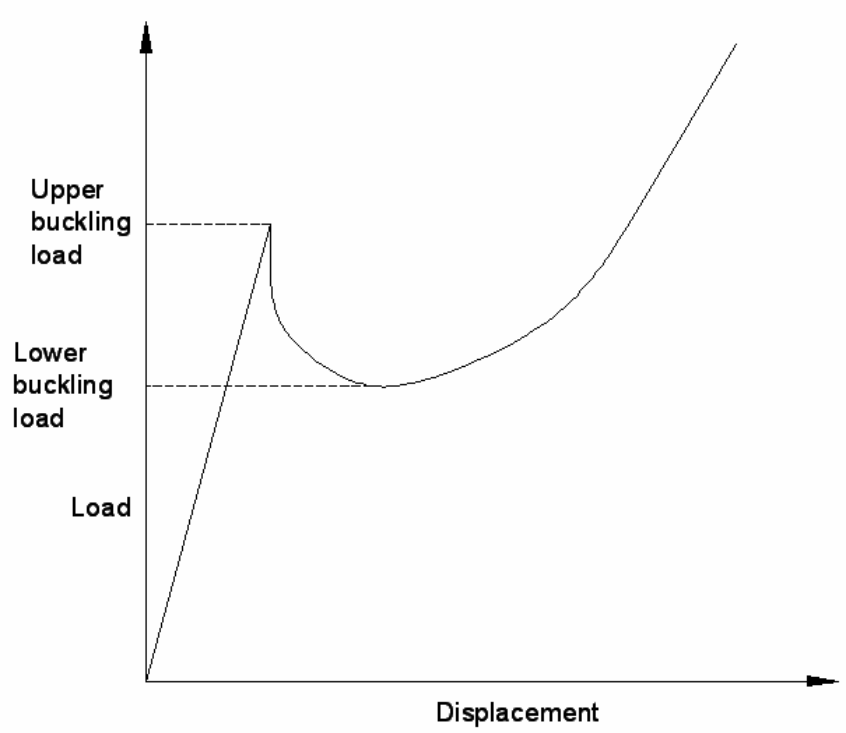

Figure 3.14: Typical load deflection curve for systems that exhibit snap buckling

The buckling load predicted by the FEA simulations is significantly higher than those obtained by experimental method. This can be attributed to the fact that during the experiments it was observed that the failure of the specimen occurred due to sudden fracture of the foam. This explains a sudden drop in the load and a sharp change in trend in the load deflection curve. Corona (2006) has stated that foams with more ductility

than Rohacell 71 but with similar stiffness would have been able to carry even higher loads before buckling. The FEA model doesn't account for the foam failure the discrepancy in the stiffness of the 10 degree model is more prominent because of the cracking of the foam near the clamped end very early during the experiment. This is quite evident from the experimental load deflection curve as the slope of this curve changes radically after a small deflection.

4. ANALYTICAL SOLUTION

Analytical models of a problem are one of the tools to obtain the solution. Analytical models have an advantage that they provide a deep insight into the behavior of the elements involved. It provides a clear picture of the interdependence of various parameters and helps in correlating the behavior with specific material and geometric properties. Thus a good model can provide a reasonable solution, good understanding of the response and further help in establishing design guidelines for the problem under consideration. However creating such models requires a thorough understanding of the problem and the solutions can be very complex. Formulating an analytical model requires that some assumptions be made to simplify the problem, and the accuracy of the solution depends on the validity of these assumptions. While formulating a problem various methodologies of analysis can be adopted. For stability analysis Gambhir (2004) has classified the approaches into two categories:

1) Equilibrium approach:

In this approach the equilibrium configuration of the system is considered. The objective is to predict the values of the loads for which a perfect system admits additional close equilibrium states referred as modes. Modes are equilibrium states with different deformation patterns (Gambhir, 2004). The problem is formulated by equating the destabilizing forces with the restoring forces and the destabilizing moments with the restoring moments. This method is generally applied for simple beam problems. Here

the total deflection is expressed as a sum of partial deflections – deflection due to bending and deflections due to shear ($w = w_b + w_s$). This necessitates the application of the compatibility conditions at the interface of the two layers. Appendix C illustrates the use of this approach for a simply supported column buckling. For more complicated problems the energy method is applied.

2) Energy approach:

The energy approach is based on the *principle of minimum potential energy* which states that a conservative system is in a configuration of stable equilibrium, if and only if, the value of potential energy s relative minimum. A *conservative system* is one in which the virtual work vanishes for a virtual displacement that carries the system around any closed path. A conservative system is in equilibrium when the energy stored is equal to the work done by external loads (Gambhir, 2004). The critical load is predicted using this criterion.

Another approach similar to the energy method is the virtual work principle. The theorem states that "If the displacements corresponding to the exact solution to the problem, with the stresses satisfying the equations of equilibrium, is perturbed by adding arbitrary virtual displacements, then the work done by the external forces along these virtual displacements equals the work done by the stresses along the corresponding virtual strains" or $\delta W_e = \delta W_i$, where W represents the work done. The equilibrium

conditions can be established from this relation. Solving these governing equilibrium equation leads to the desired results.

4.1 The energy analysis of arch buckling

In this research the energy method will be applied to the stability analysis of the arch. The energy analysis is a very effective tool for complex problems. Figure 4.1 shows the geometry of the bi-layered arch. The radial direction is along the r axis, tangential along s axis and the width of the arch is along a axis.

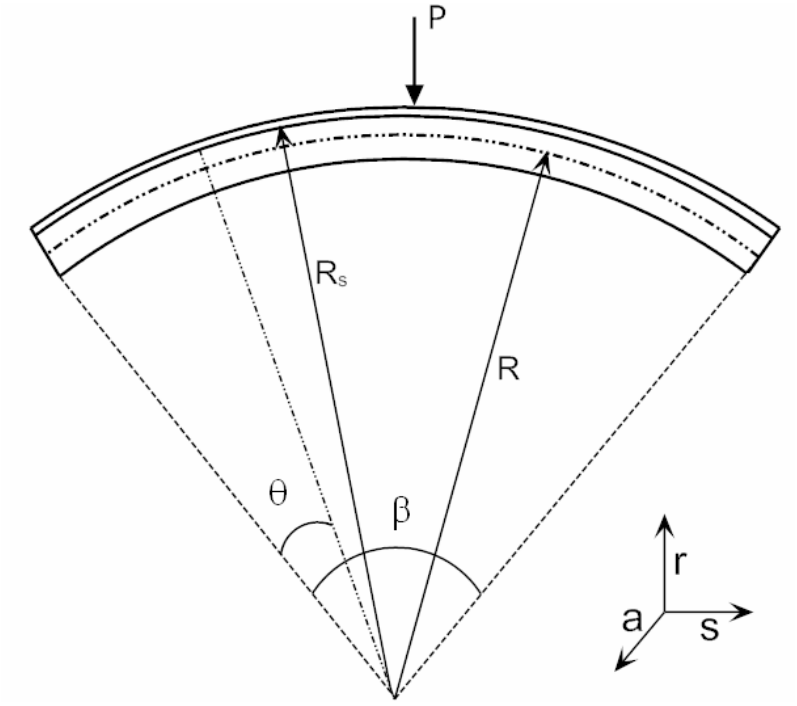

Figure 4.1: Geometrical parameters of the arch

The energy analysis model is based on the following approximations made to simplify the problem:

1) The faces are treated as thin elastic panels that follow Bernoulli assumptions.
2) The foam of thickness c is fully bonded with the faces.
3) The foam is considered to be a 2-D elastic medium with resistance to shear and radial stresses. In-plane (circumferential) stress in the foam is neglected. The explanation for this is as follows. Modern sandwich structures are made of very stiff faces (metallic or composite materials) and low strength honeycomb or foam cores. In this case of the foam is isotropic, the modulus of elasticity of the foam is three orders smaller than the modulus of the faces, while the thickness of the foam is about one order thicker than thickness of the faces. This justifies neglect of the flexural rigidity of the foam with respect to those of the faces, which, in other words, means disregard of the in-plane rigidity of the foam (Plantema, 1966).
4) The arch is shallow i.e. the initial mid-surface slope and curvature are small
5) The materials of foam and faces are isotropic.
6) All initial deflections in the pre-buckling state are small.
7) Displacement, strains and stresses in the direction perpendicular to the panel (a direction) are neglected
8) The kinematic relations of the foam are those of small deformations and therefore they are linear. Note that no a priori assumptions on the deformation

fields through the thickness of the foam are made. (Bozhevolnaya and Frostig, 2001)

The face sheet is very thin so the radial strain in the face sheet can be neglected ($\varepsilon_{rr} = 0$). For the face sheet the shear strains and hence the shear strain energy can be ignored ($\gamma_{rs} = 0$) because the faces are in effect solid beams of rectangular cross section which are shallow in proportion to their spans. Plane strain condition is assumed here which implies, $\varepsilon_{aa} = \gamma_{sa} = \gamma_{ra} = 0$, for the foam as well as the face sheet. By symmetry there are no shear stresses in the *ra* and the *sa* plane for the foam as well as the face sheet ($\gamma_{ra} = \gamma_{sa} = 0$). The normal stresses in the foam in the radial and tangential direction are negligible because the foam is assumed to be antiplane ($\varepsilon_{ss} = \varepsilon_{rr} = 0$).

An *antiplane foam* is an idealized foam in which the modulus of elasticity in planes parallel to the faces is zero but the shear modulus in planes perpendicular to the faces is finite. By this definition $E_c = 0$ and the antiplane foam makes no contribution to the bending stiffness of the beam. The strain energy due to direct stress and strain in the radial direction can be neglected because the transverse load intensity is assumed to be small and partly because the foam is assumed to be stiff in the radial direction (as in a honeycomb) (Allen 1969).

4.1a Kinematic considerations

Refer Figure 4.2 of short length ds of a bi-layered beam. It shows the section before and after deformation. A line in the cross section normal to the centerline is shown by points $abcd$. Without shear the line would have assumed position $a'b'c'd'$ and remained normal to the deformed centerline. If the foam undergoes shear the new position will be $a"b"c'd"$.

Let v be the tangential displacement and w the radial displacement. In the following analysis the subscripts have been avoided wherever possible. It will be clear from the context that any quantity such as E and G belong to the face and foam respectively. Let us denote angle $d"c'e$ by $\lambda(dw/ds)$ where λ is a coefficient which may have any value between $+1$ and $-t/c$. The value of λ is material and geometry dependent. The value $\lambda = +1$ applies when $\gamma_{rs} = 0$, in this case the arch bends as a composite beam, without shear deformation. The other extreme is $\lambda = -t/c$ when the foam is very flexible in shear.

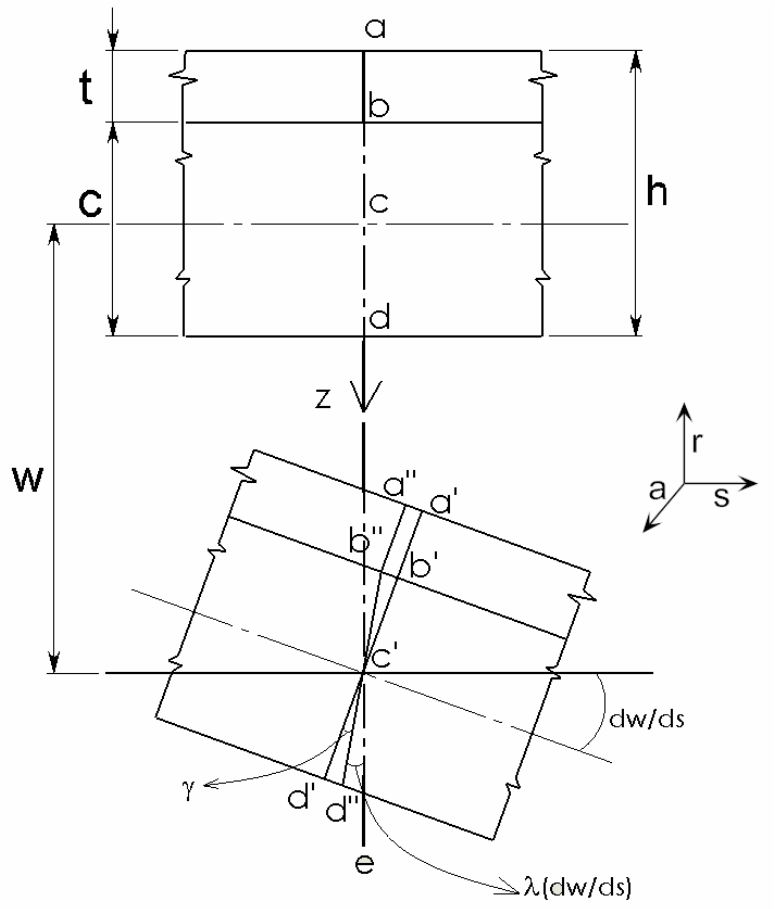

Figure 4.2: General deformation of short section of the bi-layered arch

Refer Figure .4.3 for the foam with negligible shear stiffness. The line ab rotates through an angle dw/ds to a new position $a'b'$. The point f in the mid-plane does not have any displacement in the tangential direction. Since $dd' = t/2(dw/ds)$ the angle dcd' is equal to $t/c(dw/ds)$. This angle is equal to $d''ce = \lambda(dw/ds)$ in Figure 4.2 but in the opposite sense. This gives $\lambda = -t/c$. (Allen, 1969)

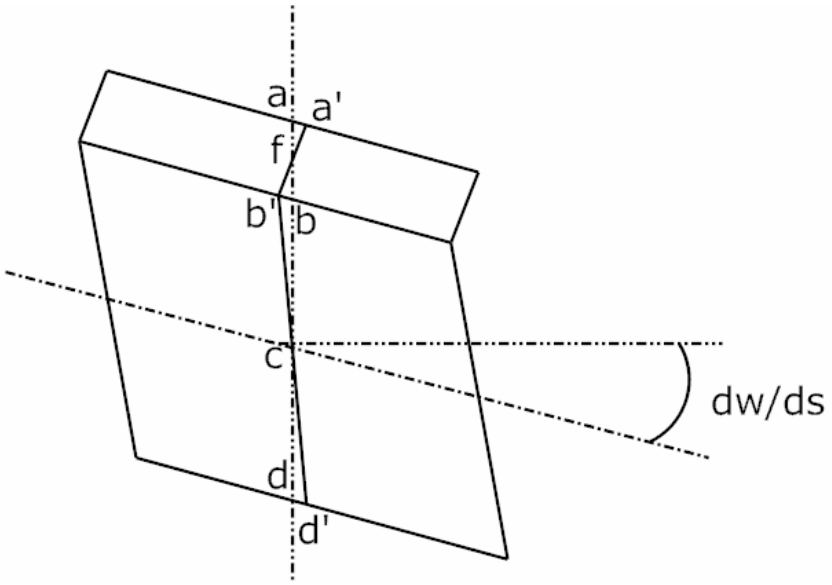

Figure 4.3: Deformation for foam with negligible core shear stiffness

4.1b Displacements in the foam and face sheet

The displacement (v) in the tangential direction of various points in the cross section can be found from the geometry of the deformed configuration $a"b"c'd"$. The equations for the displacements are as follows:

The tangential displacement in the foam ($b"d"$) is given as

$$v = -\lambda r \frac{dw}{ds} \tag{4.1}$$

where $r = R - R_s$, for $-\frac{c}{2} \le r \le \frac{c}{2}$

The tangential displacement in the face ($a"b"$) is given as

$$v = \lambda \frac{c}{2}\frac{dw}{ds} - \left(r - \frac{c}{2} \right)\frac{dw}{ds}$$

where $h = t + c$, for $-\frac{h}{2} \le r \le \frac{c}{2}$

$$v = -\left\{ \frac{c}{2}(1-\lambda) + r \right\}\frac{dw}{ds} \tag{4.2}$$

At the mid-plane of the face, $r = -\frac{c+t}{2}$, substituting this value of r in equation (4.2) gives

$$v = -\left\{ \frac{c}{2}(1-\lambda) - \frac{c+t}{2} \right\}\frac{dw}{ds} \; = \frac{1}{2}(c\lambda + t)\frac{dw}{ds} \tag{4.3}$$

The above equations have setup the displacement field in the deformed configuration. These will now form the basis for defining the strain field in the bi-layered cross section.

4.1c Strains in the foam and the face sheet

Shear strain in the foam is given by

$$\gamma_{sr} = \frac{dw}{ds} + \frac{dv}{dr} \tag{4.4}$$

Substituting $v = -\lambda r \frac{dw}{ds}$ from equation (4.1) in equation (4.4) for the foam,

$$\gamma_{sr} = \frac{dw}{ds}(1-\lambda) \tag{4.5}$$

All other strains in the foam are neglected as explained in Section 4.1.

Membrane strain in the face sheet is given by

$$\varepsilon_{ss} = \frac{dv}{ds} - \frac{w}{R} + \frac{1}{2}\left(\frac{dw}{ds}\right)^2 \tag{4.6}$$

Gjelsvik and Bonder (1962) in their research on arch buckling have shown that the membrane strain has to be constant for tangential equilibrium. Bradford et al. (2002) too has presented a similar argument. They however were not concerned with the term dv/ds as the tangential displacement v at the arch centerline was zero in their case.

Substituting for the mid-plane tangential displacement from equation (4.3)

$$\varepsilon_{ss} = \frac{1}{2}(c\lambda + t)\frac{d^2w}{ds^2} - \frac{w}{R} + \frac{1}{2}\left(\frac{dw}{ds}\right)^2 \tag{4.7}$$

4.1d Strain energy of the foam and the face sheet

The strain energy of the foam and the face sheet are to be considered individually and each is a function of the strain in the respective element.

$$U_s = \frac{G}{2}\int_{Vc} \gamma_{sr}^2 dV \tag{4.8}$$

$$U_m = \frac{E}{2}\int_{Vf} \varepsilon_{ss}{}^2 dV \tag{4.9}$$

$$U_b = \frac{E}{2}\int_{Vf} \varepsilon_b{}^2 dV \tag{4.10}$$

Substituting from (4.5) in (4.8)

$$U_s = \frac{G}{2}\iiint_{Vc} (1-\lambda)^2\left(\frac{dw}{Rd\theta}\right)^2 dsdxdr$$

$$U_s = \frac{Gfc}{2}\int_0^{\beta} \frac{(1-\lambda)^2}{R^2}\left(\frac{dw}{d\theta}\right)^2 d\theta \tag{4.11}$$

Substituting from (4.7) in (4.9)

$$U_m = \frac{E}{2}\iiint_{Vf}\left\{\frac{1}{2}(c\lambda+t)\frac{d^2w}{ds^2}-\frac{w}{R}+\frac{1}{2}\left(\frac{dw}{ds}\right)^2\right\}^2 dsdadr$$

$$U_m = \frac{Etf}{2}\left\{\int_{\theta=0}^{\beta}\left(\frac{1}{2R^2}(c\lambda+t)\left(\frac{d^2w}{d\theta^2}\right)-\frac{w}{R}+\frac{1}{2}\left(\frac{dw}{Rd\theta}\right)^2\right)\right\}^2 d\theta \tag{4.12}$$

$$U_B = \frac{Et^3 f}{24R^4}\int_0^{\beta}\left(\frac{d^2w}{d\theta^2}\right)^2 d\theta \tag{4.13}$$

4.1e Potential energy of the applied load

As can be seen from Figure 4.4 the centerline of the arch deflects under the effect of the applied load, P.

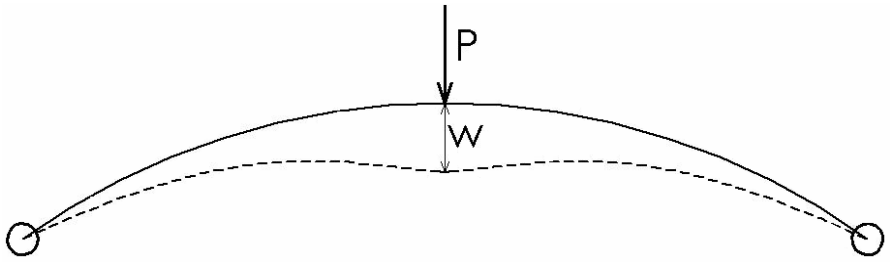

Figure 4.4: Displacement of P by w

As the arch deflects the change in potential energy of the load is given by

$$V = -Pw\Big|_{\theta=\frac{\beta}{2}} \tag{4.14}$$

4.1f Total energy (H)

The total energy of the system is the sum of the strain energies and potential energy of the load

$$H = U_m + U_B + U_s + V \tag{4.15}$$

$$H = \frac{Etf}{2}\left\{\int_{\theta=0}^{\beta}\left(\frac{1}{2R^2}(c\lambda + t)\left(\frac{d^2w}{d\theta^2}\right)^2 - \frac{w}{R} + \frac{1}{2}\left(\frac{dw}{Rd\theta}\right)^2\right)\right\}^2 d\theta + \frac{Et^3 f}{24R^4}\int_0^{\beta}\left(\frac{d^2w}{d\theta^2}\right)^2 d\theta$$

$$+\frac{Gfc}{2}\int_0^{\beta}\frac{(1-\lambda)^2}{R^2}\left(\frac{dw}{d\theta}\right)^2 d\theta - Pw\Big|_{\theta=\frac{\beta}{2}} \tag{4.16}$$

4.2 Method of solution

The total energy of the system has been expressed in terms of the geometric properties, material properties, deflections and the applied loads. There are different methods of solving this equation which have been methodically enlisted by Gambhir (2004). These are 1) The method of trial functions 2) Galerkin method 3) Finite difference method 4) Numerical integration. The trial function method has been adopted here, according to which we need to assume a function that will represent the deformed shape of the arch. The trial function presents an advantage that the boundary conditions are implemented automatically as the selected function needs to satisfy all the boundary conditions.

4.2a Assumed solution

The deformed shape can be approximated by using an infinite sine series as

$$w = \sum_{n=1}^{\infty} a_n \sin\left(\frac{n\pi\theta}{\beta}\right) \tag{4.17}$$

However the objective of the present research work is to evaluate the buckling load in the first mode. This simplifies the problem because a two term solution can be used to represent the deformed shape of the first buckling mode. A simple two term solution can be represented as:

$$w = a_1 f_1(\theta/\beta) + a_2 f_2(\theta/\beta) \tag{4.18}$$

f_1 and f_2 are functions of (θ/β) and f_1 should be symmetric and f_2 should be anti-symmetric in the span of the arch (Gjelsvik and Bodner, 1962). For the pinned ended boundary conditions we will select the assumed solution to be

$$w = a_1 \sin\left(\frac{\pi\theta}{\beta}\right) + a_2 \sin\left(\frac{2\pi\theta}{\beta}\right) \tag{4.19}$$

The boundary conditions for a pin ended arch are given by

$$w = 0 \text{ at } \theta = 0 \text{ and } \theta = \beta \tag{4.20}$$

$$w'' = 0 \text{ at } \theta = 0 \text{ and } \theta = \beta \tag{4.21}$$

It can be easily shown that the equation (4.19) satisfies these boundary conditions.

Figure (4.5) is a plot of the function (4.22) which is given by equation:

$$w = 0.2\sin\left(\frac{\pi x}{30}\right) + 0.05\sin\left(\frac{2\pi x}{30}\right) \text{ for } 0 \le x \le 30\,. \tag{4.22}$$

The assumed function has to represent the deformed shape and Figure (4.5) demonstrates that the functions of the form (4.17) represent the anticipated deflected shape of the arch under central concentrated loading.

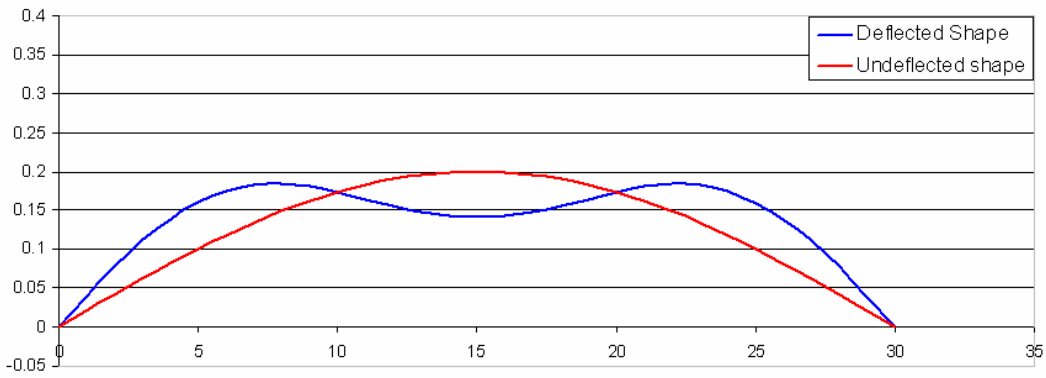

Figure 4.5: Plot of function (4.22)

Next step is to substitute the assumed solution satisfying all boundary conditions in the energy equations and minimizing the equation with respect to its variables.

4.2b Solution

Substituting for w from equation (4.19) in equation (4.16) and due to the integration results given by equation (4.23),

$$\int_0^{\beta} \sin^2\left(\frac{n\pi\theta}{\beta}\right) d\theta = \frac{\beta}{2}$$

$$\int_0^{\beta} \cos^2\left(\frac{n\pi\theta}{\beta}\right) d\theta = \frac{\beta}{2}$$

$$\int_0^{\beta} \sin\left(\frac{\pi\theta}{\beta}\right) d\theta = \frac{2\beta}{\pi} \qquad (4.23)$$

$$\int_0^{\beta} \sin\left(\frac{\pi\theta}{\beta}\right) \sin\left(\frac{2\pi\theta}{\beta}\right) d\theta = 0$$

$$\int_0^{\beta} \cos\left(\frac{\pi\theta}{\beta}\right)\cos\left(\frac{2\pi\theta}{\beta}\right)d\theta = 0$$

we can rewrite the total energy (H) as

$$H = \frac{Etf}{2}\left\{\frac{1}{2R^2}(c\lambda + t)\left(-\sum_{n=1}^{2} a_n^2\left(\frac{n\pi}{\beta}\right)^2\frac{\beta}{2}\right) - \frac{1}{R}\left(\sum_{n=1}^{2} a_n\frac{2\beta}{n\pi}\right) + \frac{1}{2R^2}\left(\sum_{n=1}^{2} a_n^2\left(\frac{n\pi}{\beta}\right)^2\frac{\beta}{2}\right)\right\}^2 +$$

$$\frac{Et^3 f}{24R^4}\left(\sum_{n=1}^{2} a_n^2\left(\frac{n\pi}{\beta}\right)^4\frac{\beta}{2}\right) + \frac{Gfc}{2}\left(\frac{1-\lambda}{R}\right)^2\left(\sum_{n=1}^{2} a_n^2\left(\frac{n\pi}{\beta}\right)^2\frac{\beta}{2}\right) - P\sum_{n=1}^{2} a_n \qquad (4.24)$$

For symmetric snap through buckling mode the anti-symmetric term has to be zero to predict a symmetrically deformed shape. This simplifies the above equation. Substituting $a_2 = 0$ leads to

$$H = \frac{Etf\beta^2}{2}\left\{\frac{(c\lambda + t)^2}{16R^4}a_1^2\frac{\beta}{2}\left(\frac{\pi}{\beta}\right)^4 + \frac{4a_1^2}{\pi^2R^2} + \frac{a_1^4\pi^4}{16R^4\beta^4} + \frac{(c\lambda + t)a_1^2\pi^2}{\pi R^3\beta^2} - \frac{(c\lambda + t)a_1^3\pi^4}{8R^4\beta^4} - \frac{a_1^3\pi^2}{\pi R^3\beta^2}\right\}$$

$$\frac{Et^3 fa_1^2}{24R^4}\frac{\beta}{2}\left(\frac{\pi}{\beta}\right)^4 + \frac{Gfca_1^2}{2}\left(\frac{1-\lambda}{R}\right)^2\left(\frac{\pi}{\beta}\right)^2\frac{\beta}{2} - Pa_1 \qquad (4.25)$$

The total energy of the system given by equation (4.24) is a function of the unknown amplitude λ and a_1. For equilibrium it is necessary that the energy should be stationary with respect to λ and a_1. Therefore,

$$\frac{\partial H}{\partial \lambda} = 0 \qquad (4.26)$$

$$\frac{\partial H}{\partial a_1} = 0 \qquad (4.27)$$

Equation (4.26) gives the value of λ as

$$\lambda = \frac{\frac{1}{2R} - \frac{t}{R^2}\frac{\pi^2}{\beta^2} + \frac{G}{Et}}{\frac{c}{R^2}\frac{\pi^2}{\beta^2} + \frac{G}{Et}} \tag{4.28}$$

Implementing the differentiation and equating to zero yields load P we get

$$P = \frac{Etf\beta^2}{2}\left\{\frac{(c\lambda+t)^2}{8R^4}a_1\left(\frac{\pi}{\beta}\right)^4 + \frac{8a_1}{\pi^2R^2} + \frac{a_1^3\pi^4}{4R^4\beta^4} + \frac{2(c\lambda+t)a_1\pi^2}{\pi R^3\beta^2} - \frac{3(c\lambda+t)a_1^2\pi^4}{8R^4\beta^4} - \frac{3a_1^2\pi^2}{\pi R^3\beta^2}\right\}$$

$$+ \frac{Et^3fa_1\beta}{24R^4}\left(\frac{\pi}{\beta}\right)^4 + \frac{Gfc\beta a_1}{2}\left(\frac{1-\lambda}{R}\right)^2\left(\frac{\pi}{\beta}\right)^2 \tag{4.29}$$

Equation (4.29) provides a good understanding of the dependence of the critical buckling load on various arch parameters. This model can be further used to conduct a parametric study of the arch behavior under different parameters.

4.3 Numerical example

Here a shallow bi-layered arch consisting of Rohacell 71 foam and aluminum faces is considered. The problem is the same as that illustrated in the experimental study in Section 3. The material properties and geometric properties are defined in Tables 4.1 and 4.2 respectively.

Table 4-1: Material properties

$E_{Al}(psi)$	υ_{Al}	$E_{Rh}(psi)$	υ_{Rh}
10^7	0.3	13100	0.35

Table 4-2: Geometric properties

R (mm)	$\beta/2$ (°)	t (mm)	c (mm)
511.81	10	1.01	12.70
342.90	15	1.01	12.70

It should be noted that there is a difference in boundary conditions for the problem in section (3.3a) and this section. Pinned boundary conditions are used in this section where as the experiment had end clamped boundary conditions. Figure 4.6 shows the comparison of the load deflection curves obtained from the analytical and the numerical technique for the same model.

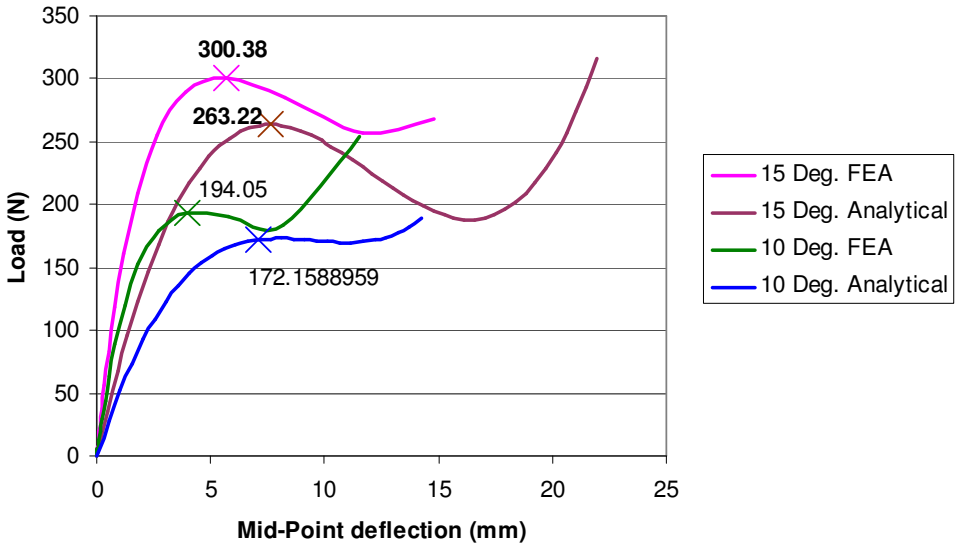

Figure 4.6: Comparison of analytical and FEA load deflection curve

It is observed that the curve from the analytical model shows a trend similar to that of the FEA model. The stiffness predicted by the analytical model is lower than that given by the FEA. The critical load predicted is 12.3 % lower than the FEA prediction.

4.4 Discussion

The analysis done here gives a conservative prediction of the critical buckling load since a non-linear term is used in the strain equation. Buckling loads traditionally obtained from classical buckling theory have given an overestimation of the critical load (Bradford, Uy, Pi, 2002).

From the comparison of the results it is observed that the analytical solution predicts a load that is 12% lower than that predicted by the FEA. This discrepancy can be partly attributed to the formulation used by the two methodologies. The FEA uses the Riks method which assumes proportional loading whereas the analytical solution uses the energy method formulation. This method calculates the critical load from the energy criterion, which predicts a critical load value called the energy load. This load is a conservative estimate of the buckling load because for snap buckling the energy load is a lower bound (Gjelsvik and Bodner, 1962).

Other factors contributing to the discrepancy between the analytical and FEA results are the assumptions made in the analytical model. The assumption of anti-plane foam in the analytical model sets the modulus of elasticity of the core to zero ($E_c = 0$). However the

FEA model does not ignore the effect of E_c. Ignoring E_c is one of the reasons that lead to a lower load prediction by the analytical model. To verify this fact the numerical simulations were done by reducing E_c and selecting a Poisson's ratio such that the shear modulus remains the same. The results from this simulation predicted a critical buckling load that was within 7% of the analytical load. Figure 4.7 shows the results for the 15 degree arch with the material properties adjusted to simulate the antiplane foam.

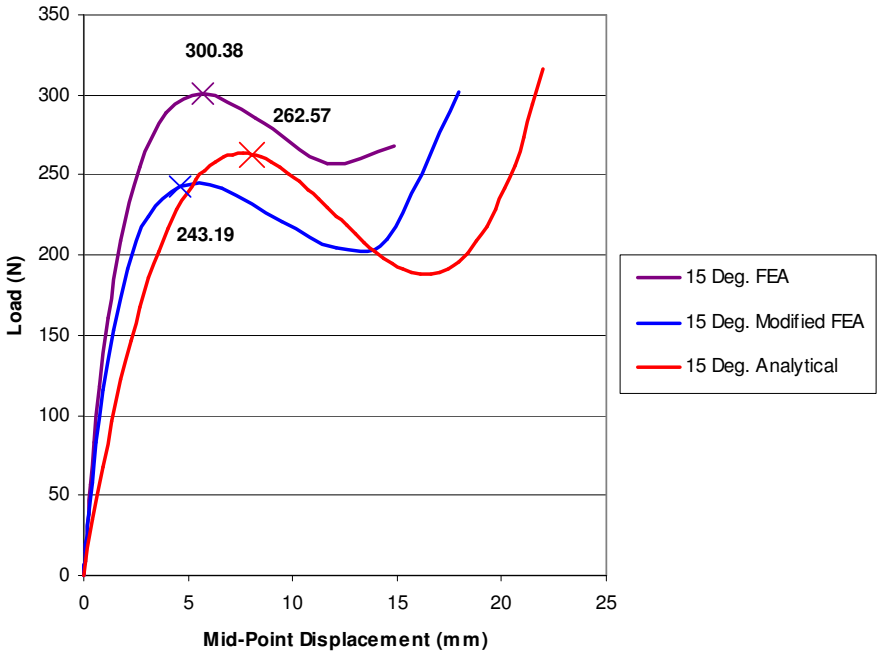

Figure 4.7: Load deflection curves for 15 degree bi-layered arch

The trial function assumed for solving the energy equation is in the simplest form – a two term solution and eventually reduced to a single term for the symmetric problem. This was done to keep the final solution simple. However to approximate the deformed

shape of the arch very accurately large numbers of terms are needed to be considered, ideally an infinite term solution is expected to give the closest approximation.

5. IMPERFECTION ANALYSIS AND PARAMETRIC STUDY

The behavior of shallow bi-layered arch under a central concentrated load was investigated in Sections 3 and 4. The main objective of this study was to determine the critical buckling load in symmetric snap through mode. It will be of great significance to study the effect of different parameters involved on the results obtained from the numerical and analytical models. Results from the numerical model (Section 3) when compared with the experimental data showed a discrepancy. One of the reasons for this, identified previously was the foam failure during the experimental investigation. Other factors to be considered are the imperfections in the experimental specimen. In the following study, the numerical model will be applied to analyze the effects of complex factors like geometrical imperfections, material non-homogeneity on the critical buckling load.

5.1 Imperfection analysis

The analytical model is based on the assumptions of homogeneous isotropic materials and perfect geometry. Thus the model cannot be employed for a more complex analysis like study of material non-homogeneity, manufacturing defects in the dimensions of the arch or imperfectly bonded layers of the core and face sheets. The FEA model can handle these kinds of complexities and can be effectively employed for this purpose. The objective of the following investigation is to study the effects of various possible imperfections on the load carrying capacity of the bi-layered arch.

5.1a Material imperfections

Material imperfections are caused due to defective manufacturing processes or due to lack of care in specimen preparation. Examples of imperfections are air or solid inclusions, non-uniform material density or imperfect bonding. As a result of the imperfection the material properties do not remain homogeneous through out the section. This hampers the materials ability to support the designated load. The effect is more pronounced in stability analysis as it can lead to an unwanted perturbation. In this analysis the effect of the material non-homogeneity on the critical load of the bi-layered arches is investigated.

Case I: Material non-homogeneity at an arbitrary location

Here the material non-homogeneity is defined at a location close to the center of the half arch. This location was arbitrarily chosen. The elements in this section were assigned a Modulus of elasticity (E) that was 10% less than the original material property. Figure 5.1 shows the location of the imperfection for this case.

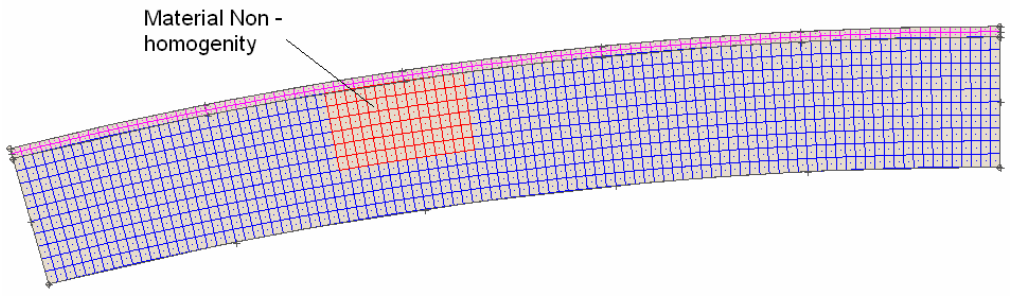

Figure 5.1: Material imperfection at the center of the half arch

Case II: Material non-homogeneity at maximum strain location in the foam

The maximum strain in the foam was found to be at the point exactly below the point of loading i.e. the center of the arch and at the point in the section farthest away from the neutral axis. In this case the material imperfection was introduced at this location. Figure 5.2 shows the location of the imperfection for this case.

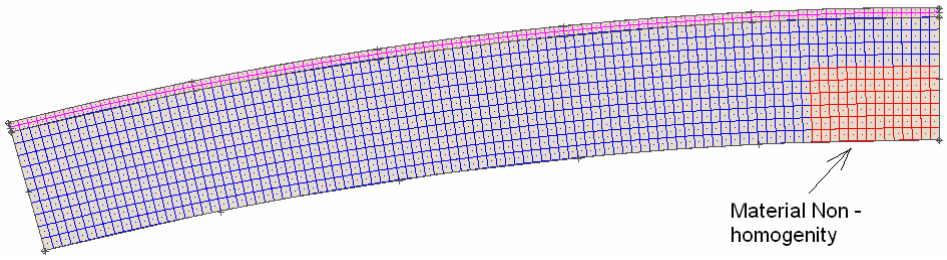

Figure 5.2: Material imperfection at the maximum strain location

It should be noted that the volume of the imperfection and the Modulus of elasticity (E) are the same for both cases. The arch used in this analysis is the same as described by Corona (2006). The arch properties have been defined previously in Section 3.

5.1b Material imperfections results

Figure 5.3 shows the load deflection curve and the critical load for the two cases of imperfections and the ideal curve when the material is without any defects. The

comparison in Table 5.1 shows that the location of the imperfection has a huge bearing on the effect it has on the load carrying capacity of the structure. The load carrying capacity deteriorates immensely if the imperfections are located at the point of maximum strain. This draws attention to the fact that care must be taken while manufacturing of bi-layered materials to obtain a good performance.

Table 5-1: Comparison of critical buckling load

Case	Critical Buckling load (N)	Error
Ideal	300.38	--
Case I	279.15	-7.06 %
Case II	178.39	-40.66 %

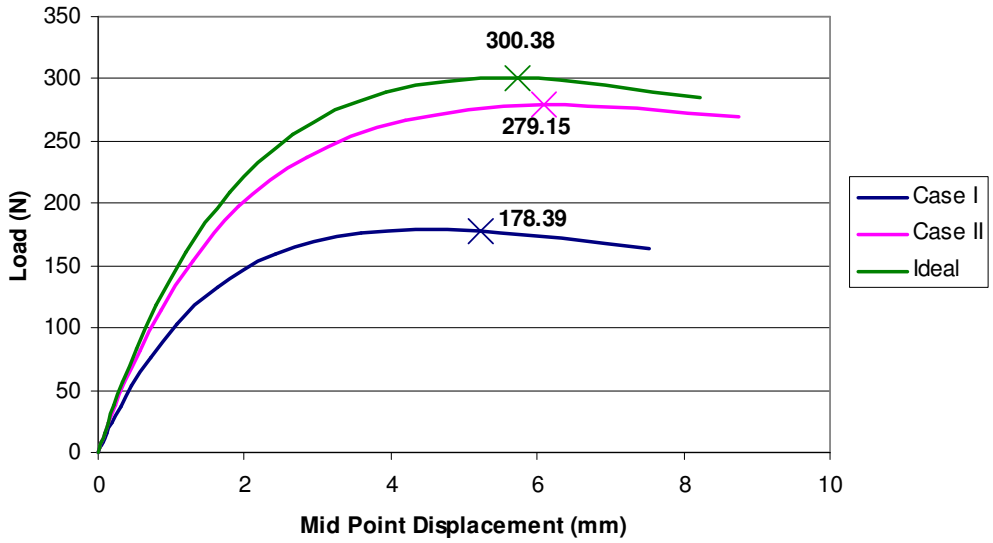

Figure 5.3: Load deflection curve for different cases

5.1c Geometric imperfections

Geometric imperfections are induced when the dimensions of the structure differ from the original design. These include certain straight segments or multiple radii instead of a singly curved structure. In this analysis a geometric imperfection has been introduced in the foam. The imperfection is shown in Figure 5.4. Figure 5.5 shows the load deflection curve for the arch with and without the imperfection. The results have been compared in Table 5.2.

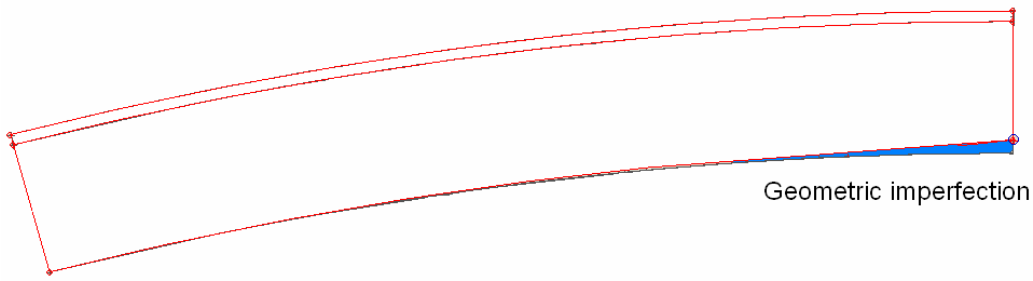

Figure 5.4: Induced geometric imperfection in foam

Table 5-2: Comparison

Case	Critical Buckling load (N)	Error
Ideal	300.38	--
With geometric imperfection	248.79	-17.19 %

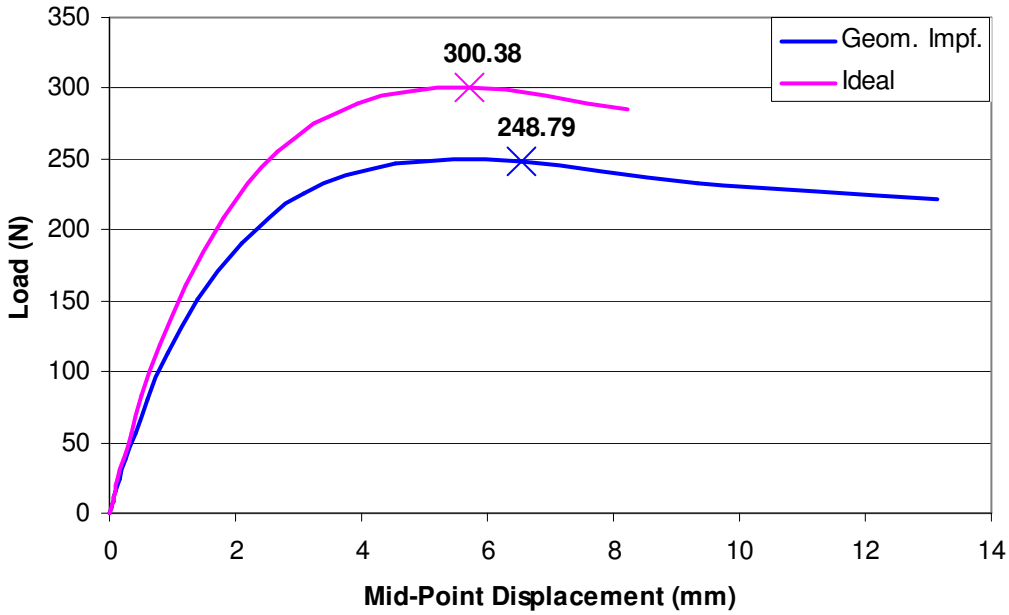

Figure 5.5: Load deflection curve for different cases

These results from the investigation of geometric and material imperfections show that these can have significant effect on the load carrying capacity of the structures. It has been shown that the presence of defects in the foam can be detrimental as the critical load comes down by a massive 40 %. These results also explain some of the discrepancies between the experimental, and the analytical and numerical results, as these effects can be seen only in the experimental investigation. This also emphasizes on the importance of good specimen preparation techniques in experimental analysis.

5.2 Parametric study

The objective of the following study is to evaluate the variation of the critical buckling load with changing arch parameters using the analytical model. MATLAB codes were used for repeated calculation of the critical buckling load (P) from equation (4.20). In each code the parameter of interest was varied keeping other parameters constant. This study was conducted for more than one set of given conditions to check for the consistency of the trend.

5.2a Effect of foam thickness to face sheet thickness ratio, (c/t)

In this study keeping all the geometric and material properties same, the ratio of thickness of the core to the thickness of the face sheet (c/t) is varied to study the change in critical load with the changing ratio. Fig 5.6 shows the plot of critical load versus the c/t ratio for two different cases. On expected lines the, the critical buckling load increases with the increase in this ratio. This increase in critical load however is less prominent at lower ratios. The thickness of the core starts assuming a greater importance at higher thicknesses.

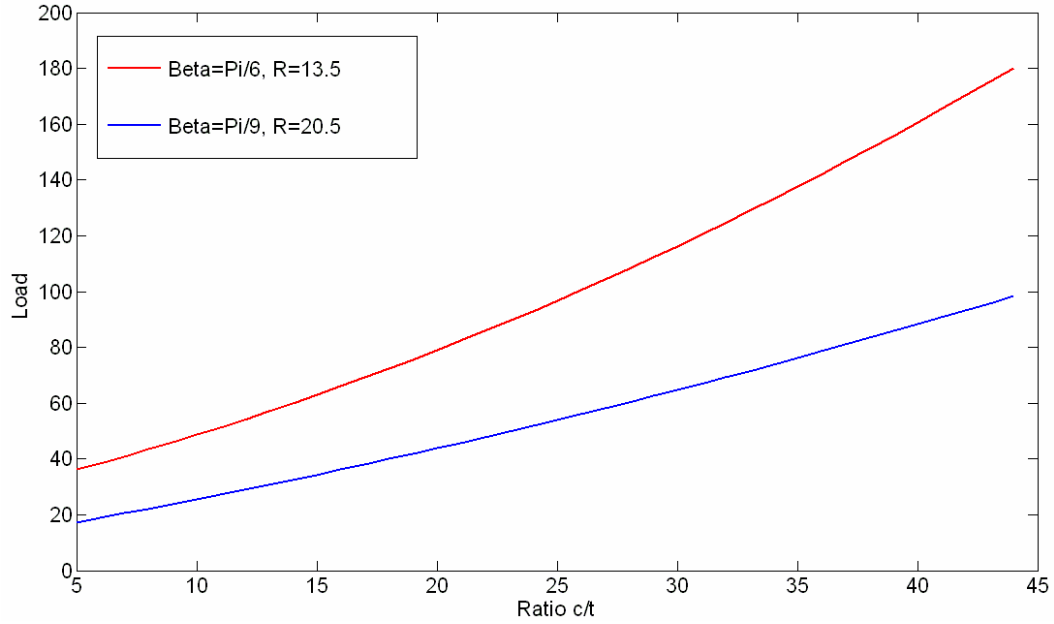

Figure 5.6: Variation of critical load with c/t ratio

5.2b Effect of radius, (R)

In this study keeping all the geometric and material properties the radius of the arch (R) is varied to study the change in critical load with the changing radius. Figure 5.7 shows the variation of critical load with the radius of the arch. Three different cases of included angle are shown in the figure. The trend shows that for a given included angle increase in the arch radius will reduce the load carrying capacity of the arch. This can be attributed to the fact that the shallow arch will approximate a flat panel as the radius tends towards infinity and the reaction force to support the lateral loads proportionally decreases.

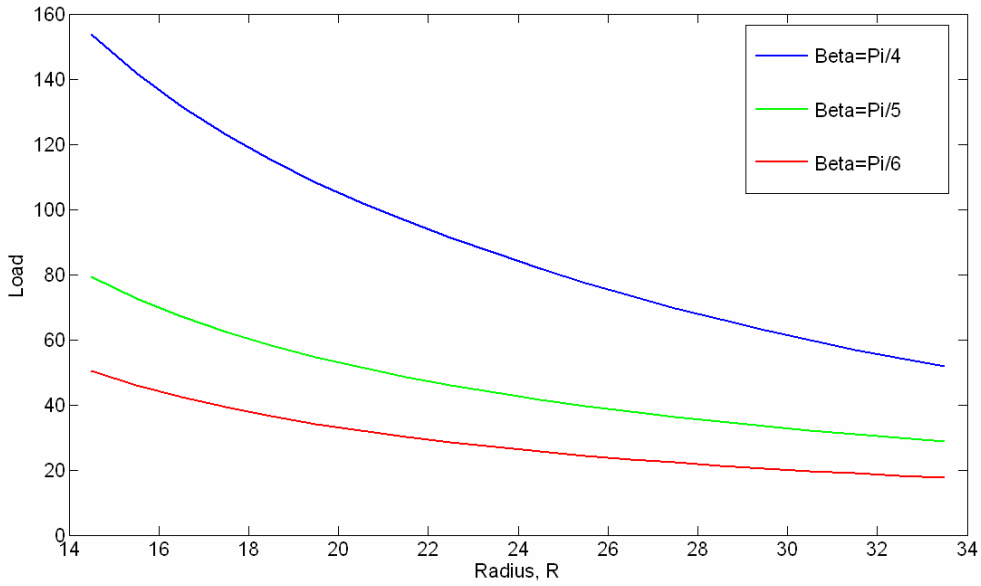

Figure 5.7: Variation of critical load with R

5.2c Effect of included angle, (β)

In this study keeping all the geometric and material properties the included angle of the arch (β) is varied to study the change in critical load with the changing angle. Figure 5.8 represents the trend of critical load with increasing subtended angle for three different radii. The formulation used here is valid only for shallow arches and hence this study considers included angles only up to 90 degrees which fall into our definition of shallow arches. The trend shows that for a given radius the load carrying capacity increase almost linearly with the included angle.

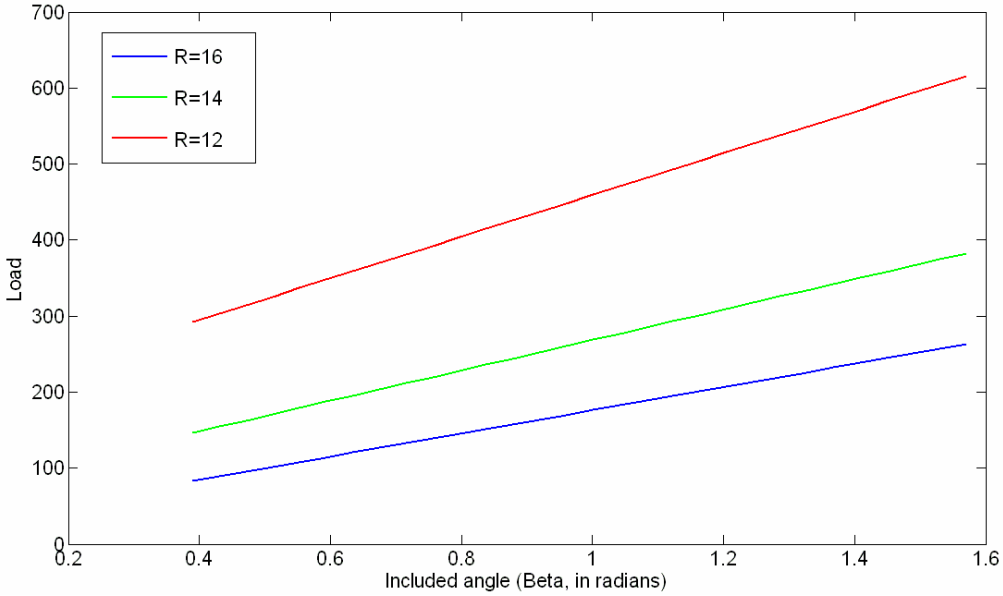

Figure 5.8: Variation of critical load with included angle

5.2d Constant spans

In this study the span (S) and the material properties are maintained constant and the included angle (β) and the radius of the arch is varied accordingly to study the change in critical load. Figure 5.9 shows the trend of critical load when the span of the arch is maintained constant against the included angle. As seen from the figure the plots of load versus the included angle for a given span tops out at an included angle of 90 degrees (1.57 radians) for a constant span.

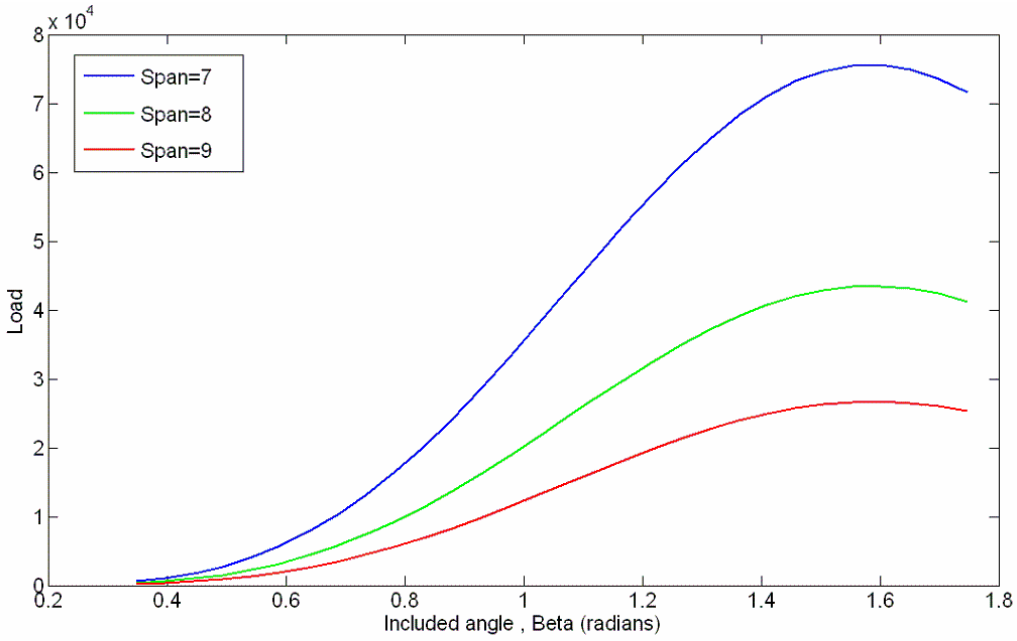

Figure 5.9: Variation of critical load with included angle and constant spans

5.2e Load deflection response

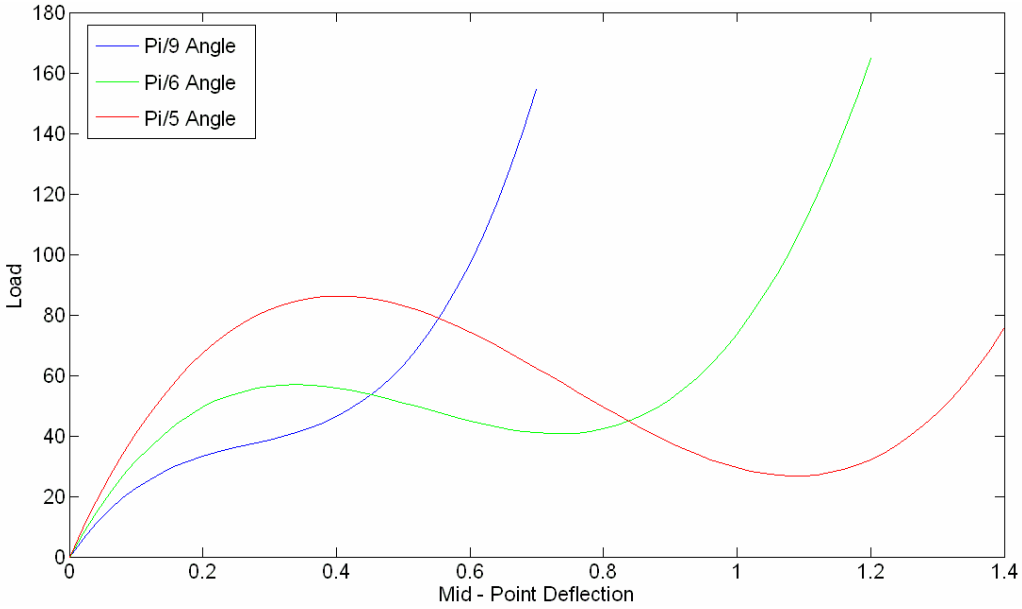

Figure 5.10: Different load deflection response

Figure 5.10 shows the load deflection responses for arches with different degree of shallowness. For arches with very small included angle it is observed that snap buckling doesn't occur because the arch extension takes place immediately after a very small deflection.

5.2f Weight reduction study

In the following analysis the weight reduction potential of bi-layered structures is demonstrated by replacing a single layer arch structure by an equivalent bi-layered structure options. The problem under study is the problem analyzed by Corona (2006) the results for which have been shown in section (3.1c). Bi-layered arch structures with different c/t ratio and having the same load carrying capacity as the single layered were designed. Figure 5.11 shows the plot of weight of the structures for different ratios. The terms in the bracket are the face sheet thickness (t) and the percentage reduction in weight respectively. The percentage value is with respect to the weight of the single later arch.

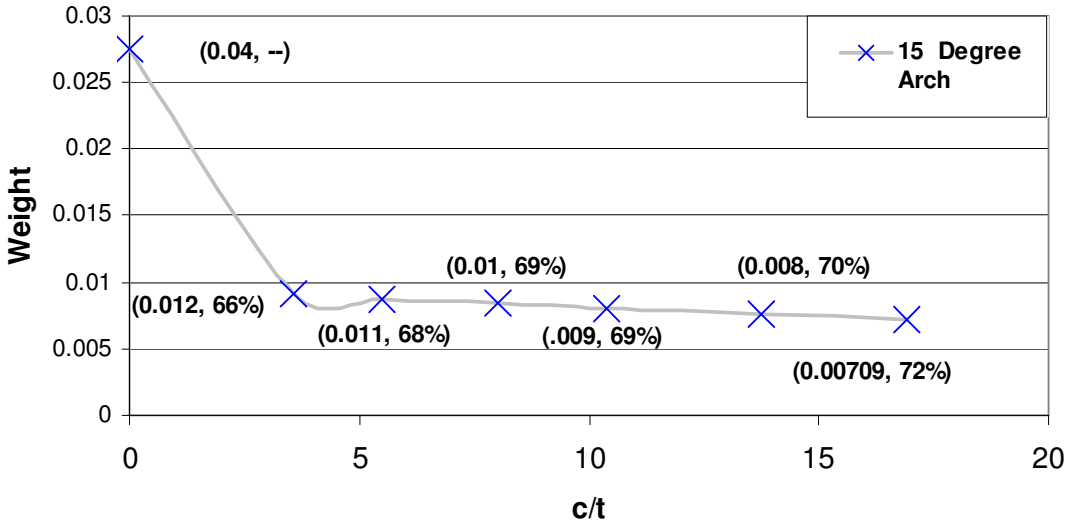

Figure 5.11: Weight vs. (c/t) for different design options

The parametric study conducted here provides insight into the arch behavior when different parameters are changed. It can be applied to establish guidelines for designing shallow bi-layered arches.

6. CONCLUSION

This research presented work on stability analysis on bi-layered materials. The objective was to investigate the buckling of shallow bi-layered arch under a central concentrated load and find an approximation to the critical buckling load. A numerical technique and an analytical technique were used to solve the problem.

The numerical technique was implemented using the ABAQUS FEA package. The FEA model was developed initially for a single layer arch and then a bi-layered arch. Numerous simulations were run to verify the correctness of the model

Energy method analysis was implemented to determine the critical buckling load analytically. The equations were solved using a trial function method. The analytical model was developed with small deflection theory and thus it is expected to provide a good approximation of the pre-buckling state and the critical buckling load. Though the initial objective was to study the pre-buckling behavior determination of the point of loss of stability the trend of the solution beyond the critical load was satisfactory. From the load deflection curves it is observed that when the load deflection plot is extended beyond the critical point the trend of this curve is of a typical symmetric snap through buckling curve. The constant increment of the load in the post buckling zone is on expected lines because as the arch deflects beyond the point of the line joining the two end points i.e. as it become concave. The load rises as it is no longer in compression and

the extension of the arch takes place. The accuracy of the points of inflection in the post buckling state as predicted by this model can be a point of further investigation.

The results from the analytical solution and the FEA model were in good agreement. The difference was observed to be around 12 %. The results predicted from the FEA were higher than that by the analytical model. The models were further verified by comparing the results with the experimental data available from Corona (2006). The results for the single layer arch buckling under a similar loading and boundary conditions were thoroughly investigated and compared with the experimental data. These results were in very close agreement.

Parametric study was conducted to investigate the effects of various arch parameters on the behavior of the arch. These can be used as guidelines for the design of the shallow bi-layered arches. The effect of geometric and material imperfection on the performance of the arch was analyzed. The results clearly showed that these can have significant detrimental effect on the structural performance.

In practical applications the real life structures are not perfect. Imperfection can be caused because of different reasons like inhomogeneous materials, geometric imperfections or imperfect bonding. Such imperfections can affect the stability of the structure and lead to premature collapse at loads significantly lower than the predicted load. The analytical model presented in this analysis is incapable of taking into account

the structural or material imperfections and predicting the consequential failure points. However the numerical model was used to investigate the effects of imperfections.

6.1 Future potential

The model developed here is for a simple bi-layered structure arch in which the material properties are isotropic and the arch is singly curved. However, this energy model for the arch can form a base for an analysis of a more complex bi-layered structure – structures having anisotropic properties. This can be done by adding more strain energy terms to the energy equation and using the relevant material properties for each term. The model can be further updated to analyze the buckling behavior of a sandwich arch under similar loading and boundary conditions. Additional strain energy due to the presence of the second face sheet needs to be considered for this analysis. Thus the model built herein is quite flexible and has further scope for enhancement.

The solution was obtained by using a simple two term solution. The accuracy of the solution can be improved by using more terms for the solution. This will require an implementation of a numerical technique using the Newton-Raphson method to solve the set of resulting non-linear simultaneous equations.

Very little data is available about stability analysis of a bi-layered arch and the buckling loads. This has left a void about the actual physical behavior of this structure under the given loading and boundary conditions. This presents an opportunity for conducting

experiments on bi-layered arch buckling. The experimental data can be used to validate the analytic and the FEA techniques.

The numerical model can be made more complex by modeling the adhesive layer between the foam and the face sheet. The existing model can be used for this purpose. This model will be a useful tool when comparing the results with experimental data as it can account for practical phenomenon like imperfectly bonded foam and face sheet or adhesive failure.

.

REFERENCES

ABAQUS Users manual, 2007. ABAQUS online documentation. http://sc.tamu.edu:2080/v6.5/ books/stm/default.htm

Alfutov, N. A., 1999. Stability of elastic structures. Springer, New York.

Allen, H. G., 1969. Analysis and design of structural sandwich panels. Pergamon Press, Oxford.

Bazant, P. Z., 1989. Stability of structures. Dover Publications, Inc, New York.

Bozhevolnaya, E., Frostig, Y., 2001. Free vibrations of curved sandwich beams with a transversely flexible core. Journal of Sandwich Structures and Materials 3, 47-73.

Bradford, M.A., Uy, B., Pi, Y.L., 2002. In-plane elastic stability of arches under a central concentrated load. Journal of Engineering Mechanics, ASCE 128 7, 710–719.

Bull, P. H., Hallstrom, S., 2004. Curved sandwich beams with face–core debond subjected to bending moment. Journal of Sandwich Structures and Mechanics 6 (2), 115-127.

Corona, E., 2006. Buckling of a shallow bi-layered arch. Unpublished research data.

Dickie, J. F., Broughton, P., 1971. Stability criteria for shallow arches. Journal of Engineering Mechanics Division EM3, 951 – 963.

Dym, C. L., 1973. Bifurcation analysis for shallow arches. Journal of Engineering Mechanics Division EM2, 287-301.

Dym, C. L., 1974. Stability theory and its application to structural mechanics. Noordhoff International Publishing, Leyden-Massachusetts.

Gambhir, M. L., 2004. Stability analysis and design of structures, Springer publication, New York.

Gjelvik, A., Bodner, S.R., 1962. The energy criterion and snap buckling of arches. Journal of Engineering Mechanics Division 88 (EM5), 87 – 134.

Gregory, M., 1967. Elastic instability: Analysis of buckling modes and loads on framed structures, First edition. E. & F. N. Spon Limited, London

Mahfuz, H., Islam, S., Saha, M., Carlsson, L., Shaik J., 2005. Buckling of sandwich composites; Effects of core–skin de-bonding and core density. Applied Composite Materials 12, 73-91.

Heder, M., 1991. Buckling of sandwich panels with different boundary conditions - A comparison between FE-analysis and analytical solutions. Composite Structures19, 313 – 332.

Lee, H. J., Lee, J. J., 2000. A numerical analysis of the buckling and postbuckling behavior of laminated composite shells with embedded shape memory alloy wire actuators. Smart Material Structures 9, 780 – 787.

Kerr, A. D. and Soifer, M. T., 1969. The linearization of the prebuckling state and its effect on the determined instability loads. Journal of Applied Mechanics 36 (4), 775-783

Knight Jr., N. F., Carron, W. S., 1997. Static collapse of elastic circular arches. AIAA Journal 35(12), 1876-1880.

Langhaar, H.L., Boresi, A. P., Carver, D. R., 1954. Energy theory of buckling of circular elastic rings and arches. Proceedings of the Second US National Congress of Applied Mechanics (ASME), 437 – 443.

Lyckegaard, A., Ole Thybo Thomsen, 2006. Nonlinear analysis of a curved sandwich beam joined with a straight sandwich beam. Composites Past B: Engineering 37, 101 – 107.

Plantema, F. J., 1966. Sandwich construction. John Wiley and Sons, New York.

Purdue Webpage, Constructability, maintainability, and operability of FRP bridge deck panels, http://web.ics.purdue.edu/~ohe/SPARC/JTRP/JTRP%20summary.htm, 2007

Pytel, A., Singer, F. L., 1987. Strength of materials. Harper-Collins Publishers, New Delhi.

Rajasekaran S. and Padmanabhan S., 1989. Equations of curved beams. Journal of Engineering Mechanics 115, 1094-1111.

Rose, C. A., Moore, D. F., Knight, Jr. N. F., Rankin, C. C., 2002. Finite element modeling of the buckling response of sandwich panels, AIAA 1517, 1-19.

Schreyer, H. L., Masur, E. F., 1966. Buckling of shallow arches, Journal of Engineering Mechanics Division, EM4, 1-19.

Shames, I. H., Dym, C. L., 1985. Energy and finite element methods in structural mechanics. Hemisphere Publishing Corporation, Washington.

Skvortsov, V., and Bozhevolnaya, E., 1997. Overall behavior of shallow singly-curved sandwich panels. Composite Structures 37 (1), 65-97.

Skvortsov, V., Bozhevolnaya, E., 2001. Two-dimensional analysis of shallow sandwich panels. Composite Structures 5, 43-53.

Stack Taikidis, W. J., 1972. Nonlinear buckling of cylindrical shells. Computers and Structures, 2. 615 – 624.

Timoshenko, S., 1936. Theory of elastic stability, First edition. McGraw- Hill Book Company, Inc, New York.

Unistates Webpage, April 2007.
http://unistates.com/rmt/explained/glossary/rmtglossaryb.html

U.S. Department of Transportation – FHWA, April 2007. http://www.fhwa.dot.gov/

Zenkert, D., 1995. An introduction to sandwich construction. Chameleon Press, London.

APPENDIX A

DETAILS OF THE FEA MODEL

A finite element model can predict good results if it can replicate the actual physical model as close as possible. This requires setting up various aspects of the model. The various aspects of the finite element model which need to be established are as follows,

a) Boundary conditions

b) Loading conditions

c) Element type

d) Riks method input parameters

FEA Model

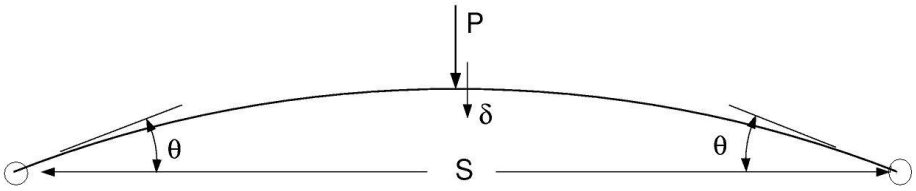

Figure A.1: Schematic

Schematically the problem configuration can be represented as shown in Figure A.1. The shallow circular arch is pinned at the two ends and loaded at the point of symmetry. The boundary conditions are also symmetric, i.e. both ends have similar (pinned) boundary condition. Exploiting this symmetry of the structure only half of the arch can be

modeled. This would not have been possible had one of the boundary conditions been pinned and other clamped. Figure A.2 shows the schematic half model of the arch.

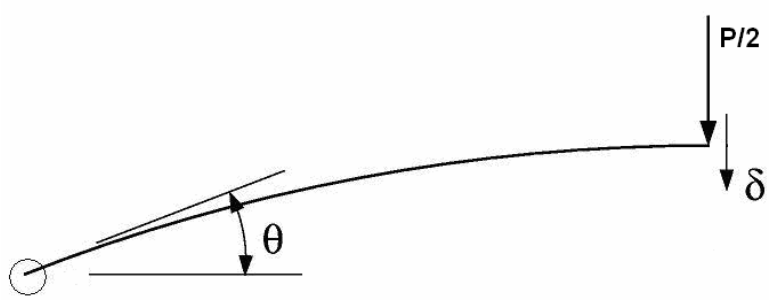

Figure A.2: Schematic of half arch exploiting the symmetry of the model

When only the half arch is modeled the physical boundary conditions cannot be applied directly. The modified boundary conditions are explained later in the boundary conditions section. One of the fundamental assumptions in solving this problem is the plane strain condition (Refer Section 6). Thus we can take advantage of the plane strain condition and model the arch as a 2 dimensional entity. The results will vary linearly with the depth of the arch in the x direction. The symmetry of the model and plane strain condition adds two simplifications to the model. This will help keep the number of elements required to model the geometry to bare minimum and make it computationally efficient.

Boundary conditions

For the clamped ends the 3 degrees of freedom of displacements and the 3 degrees of freedom of rotation are constrained. This can be implemented by using the "ENCASTRE" boundary condition from ABAQUS.

The required inputs for this keyword are

- Node number or Node set of boundary nodes

However since only the half arch is being modeled here the clamped boundary condition will appear only on one of the end. The boundary condition at the loaded end is different from clamped to implement the symmetry model. As seen in Figure 3.4 the point of symmetry under the load P/2 is free to move in the radial direction. However its displacement in the tangential direction has to be constrained. The cross section has to be constrained to rotate about the x direction. This can be explained from the fact that the presence of the other half structure of the arch would have imposed these inherent constraints on the movement of this end of the arch. These end conditions can be implemented by imposing the "XSYMM" boundary condition from ABAQUS. Thus schematically the physical model of the half arch would be as shown in Figure A.3.

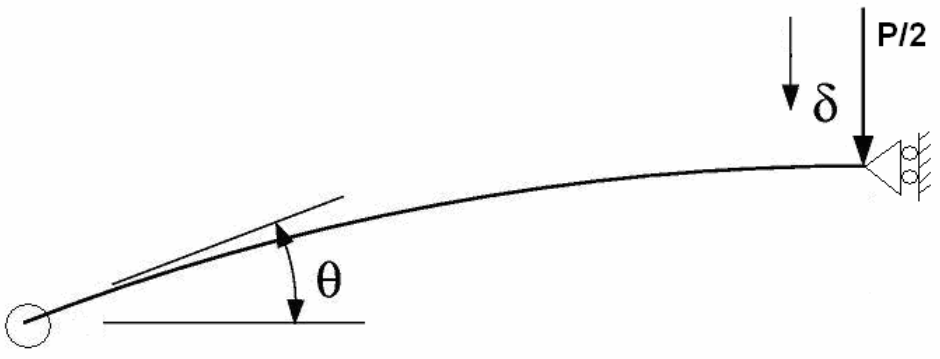

Figure A.3: Schematic of the symmetrical model

Pinned End boundary condition

One major difference between the clamped end and pinned end boundary condition is that the cross section is free to rotate in the later case where as in the former it is constrained to rotate. The pinned end condition is implemented by constraining the 3 degrees of freedom of displacement and the 2 degrees of freedom of rotation about the y and the z axes.

Loading conditions

The arch is loaded by a concentrated load at the center. A concentrated loading condition has been established by using the "CLOAD" keyword from ABAQUS. The required input for this keyword are

- The node number of the point of action of the load
- Degree of freedom
- Load magnitude

Element type

Plane-strain elements CPE4, CPE6 and CPE 8 available in ABAQUS give rise to results very close to those generated by otherwise adopting 3-D continuum elements. Since plane-strain elements are less computationally expensive than 3-D elements, they were utilized here.

Nonlinear quasi-static analysis

The stability analysis was done using the modified Riks algorithm. The analysis step required to implement this method is "STATIC RIKS". The input parameters required to implement this step are

1. Initial increment in arc length along the static equilibrium path in scaled load-displacement space, Δl_{in}. If this entry is zero or is not specified, a default value that is equal to the total arc length of the step is assumed.
2. Total arc length scale factor associated with this step, l_{period}. If this entry is zero or is not specified, a default value of 1.0 is assumed.
3. Minimum arc length increment, $\Delta l_{\min}$. If this entry is zero, a default value of the smaller of the suggested initial arc length or 10^{-5} times the total arc length is assumed.
4. Maximum arc length increment, $\Delta l_{\max}$. If this value is not specified, no upper limit is imposed.
5. Maximum value of the load proportionality factor, λ_{end}. This value is used to terminate the step when the load exceeds a certain magnitude.
6. Node number at which the finishing displacement value is being monitored.
7. Degree of freedom being monitored.
8. Value of the total displacement (or rotation) at the node and degree of freedom that, if crossed during an increment, ends the step at the current increment.

APPENDIX B

MESH SENSITIVITY ANALYSIS

Mesh sensitivity analysis is presented in the following study to determine the optimum element density.

Importance of element size

Another parameter of the finite element model which hasn't been dealt with till now is the element size. The results from a finite element analysis depend on the number of factors. One of the parameter that can affect the results significantly is the mesh. In the finite element method the domain is represented as a collection of a finite number of sub domains. This is the process of discretization of the domain into smaller units called elements. The collection of these elements is what we refer to as the finite element mesh. In the mesh the elements are connected to one another at the nodes. The results vary drastically on the type of element. In fact choosing the right kind of elements for a given problem is of fundamental importance for the success of any finite element model. However once the right kind of element is chosen for the given problem the importance of the mesh density takes over. The element size or the mesh density can affect the result in different ways. The reason for this can be attributed to the manner in which the process of finite element problem solution works. Discretization of the domain into as many sub domains as possible provides the part solutions at more number of locations and hence the whole solution will approximate the real model more closely. Thus an infinitely divided domain will give the closest answer. However in practical applications

it is not possible to divide the domain into infinite elements and the best possible option is to have a large number of elements to get a good answer. But there has to be a limit set on this number and how small the element should be or on the element density value. This is because for practical problems in stress analysis the solution is complex and the computational time is high. The computational time and the memory required to store the generated data increases directly with the number of element.

Mesh sensitivity analysis

The objective of the following study is to gauge the effect of mesh density or the element size on the results obtained for the buckling problem of bi-layered arch. As stated in the discussion above the results are expected to improve with the fineness of the mesh, but the point of interest is optimization of the resources without compromising the quality if the results.

A model of a shallow bi-layered arch is made with Aluminum for the face sheet and Rohacell as the foam and with the following specifications:

Table B.1: Geometry

R (mm)	β (°)	t (mm)	C (mm)
100	60	1	8

Table B.2: Material properties

$E_{Al}(N/mm^2)$	υ_{Al}	$E_{Rh}(N/mm^2)$	υ_{Rh}
73001	0.3	1700	0.35

Boundary condition: Fixed end boundary condition is applied on both the ends of the arch

Procedure / Methodology

A number of simulations were run using the same model. The mesh density was varied keeping rest of the simulation parameters same. Starting with a coarse mesh of element size 5 the element size was reduced with each subsequent simulation. Simulation runs were taken for element sizes of 5, 2.5, 1.5, 1, ½ and 1/3. For the first 4 cases only the foam was modeled with multiple layers of elements, whereas the face sheet was represented by a single layer of elements. From the fifth simulation ie element size ½ onwards even the face sheet was represented by multiple element layers. Effort was made to keep the elements as close to the perfect square so that the mesh remains uniform. This was done using the element size option instead of the element density option in Hypermesh.

The result of interest in this study was the buckling load of the sandwich arch. The reaction force at the supports is plotted against the displacement of point of loading. Figure 7B.1 shows the load deflection curve for the six different cases mentioned above.

The first maximum of each curve represents the critical buckling load for that particular case. It is observed that for a coarse mesh ie element size 5 shown by Series 1 the load values is quite high as compared to successive smaller element sizes. The buckling load decreases with each simulation as the mesh density is increased progressively. This observation is on expected lines because we anticipate the structure stiffness to reduce with smaller element sizes or with the mesh getting finer.

The change in the result is significant for the first three series. However after this the solution starts converging and the percentage change in the value of load is not significant. As seen from the Table 7B.3 there is only 1 % change in the value between element size 1/3 and ¼. The computation time for mesh as in series 7 is significantly higher and the memory allocation for this task is also enormous. This makes it apparent that the mesh configuration reaches its optimum state at element size 1/3 and there is no significant gain in terms of the quality of the result by refining the mesh beyond this point. As explained earlier this mesh configuration with element size 1/3 includes the core modeled as multiple element layers of element size 1 and the face sheet modeled by using element size 1/3. Thus from these observation it is incurred that the element size of '1' will provide sufficient accuracy and it will be used for further analysis.

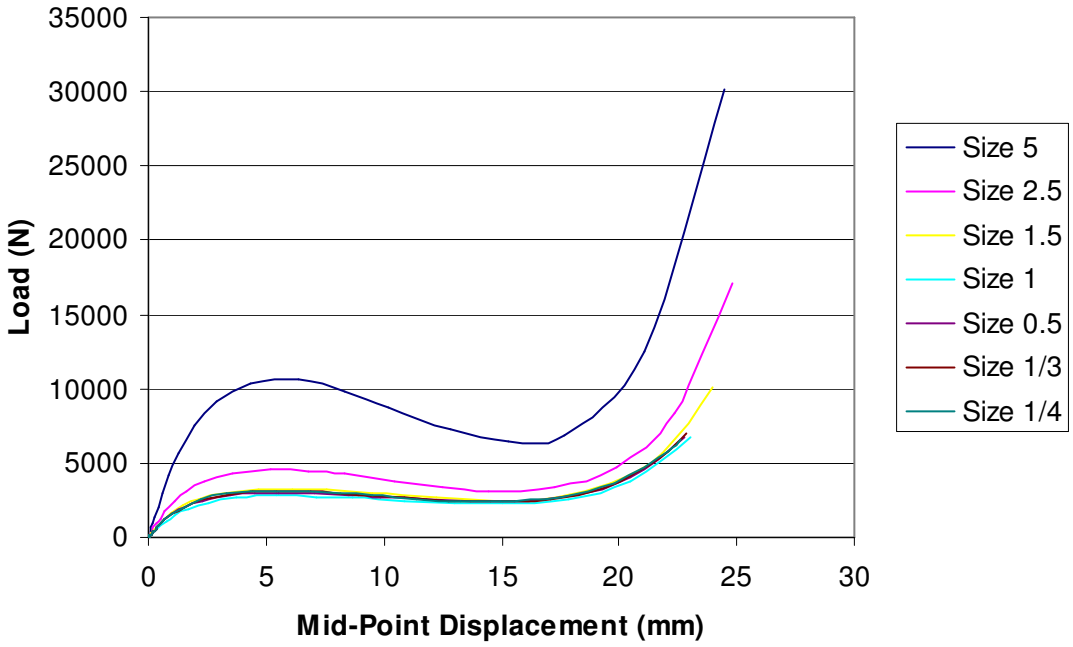

Figure B.1: Load deflection curves for different mesh sizes

Table B.3: Comparison of critical loads

Series	Element	Critical load (N)	%
1	5	10587	--
2	2.5	4590	56.64
3	1.5	3274	28.65
4	1	2779	15.12
5	1/2	3019	-8.61
6	1/3	3110	-3.01
7	1/4	3141	-1.00

APPENDIX C

EQUILIBRIUM APPROACH

The problem of in-plane buckling of a sandwich column has been used here to demonstrate the application of the equilibrium approach to solve the stability problems.

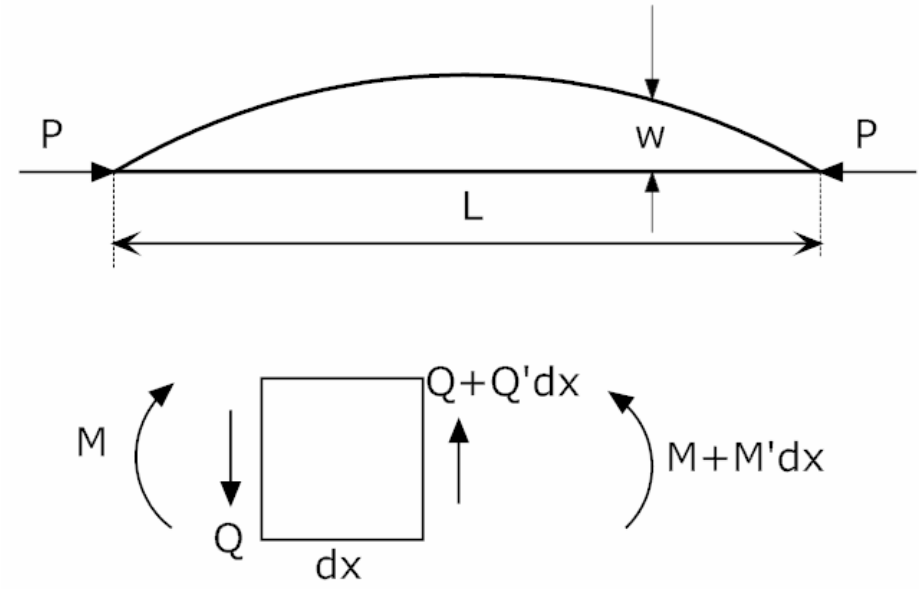

Figure C.1: Simply supported column

Figure C.1 shows a simply supported columns under axial compression and the equilibrium diagram of a small section of length dx in the column the equation of equilibrium can be written as follows

$$M = -Pw \tag{C.1}$$

$$Q = Pw' \tag{C.2}$$

Substituting these values in the governing equation gives

$$w'' + a^2 w = 0 \tag{C.3}$$

Where

$$a^2 = \frac{P}{B(1-P/S)} \tag{C.4}$$

The solution of this equation is given by

$$w = C_1 \sin ax + C_2 \cos ax \tag{C.5}$$

The boundary conditions are that $w = 0$ at $x = 0 \,\&\, x = L$. This gives $C_2 = 0$ and the stability criteria as $\sin aL = 0$. The buckling load corresponds to values $a = n\pi / L$.

Critical buckling load is given by $P = \dfrac{n^2\pi^2 B / L^2}{1 + n^2\pi^2 B / L^2 S}$

This example demonstrated the use of equilibrium approach to solve buckling problems.

APPENDIX D

ABAQUS PROGRAMS

The ABAQUS programs used in the numerical analysis are presented in this section. The node and element definition have been omitted from the original programs.

Program I: The following is the program for a single layer arch buckling problem described in section 3.1 for the arch with thickness 12.7 mm

==========

** ABAQUS Input Deck Generated by HyperMesh Version : 6.0

** Generated using HyperMesh-Abaqus Template Version : 6.0

** Template: ABAQUS/STANDARD 2D

*NODE

1, 0.0 , 0.0

2, -32.153 , 120.0

3, 0.0 , 120.0

…….

*ELEMENT,TYPE=CPE4,ELSET=al

1, 8, 313, 314, 7

2, 7, 314, 5, 6

3, 313, 306, 307, 314

……

*solid section,elset=al, material=aluminum

```
1
*Nset, nset=loadingnode
6
*nset,nset=symm1
4,5,6
*Nset, nset=fix1
157
*Material, name=aluminum
*Elastic
420000, 0.35
*Boundary
symm1, XSYMM
*Boundary
fix1, pinned
*Step,nlgeom
*Static, riks
0.01,0.2,,,,loadingnode,2,-5
*Cload
loadingnode, 2, -10.0
*Restart, write, frequency=1
*Output, field, variable=PRESELECT
*Output, history, variable=PRESELECT
```

*Output, history

*Node Output, nset=fix1

RF2

*Node Output, nset=loadingnode

U2

*End Step

==========

Problem 2: The following is the program for a bi-layered layer arch buckling problem described in section 3.3 for the arch with 15 degree included angle.

** ABAQUS Input Deck Generated by HyperMesh Version : 7.0

** Generated using HyperMesh-Abaqus Template Version : 7.0

**   Template: ABAQUS/STANDARD 2D

*NODE

** Node definitions

*ELEMENT,TYPE=CPE4,ELSET=al

** Face sheet element definition

*ELEMENT,TYPE=CPE4,ELSET=fm

**Foam element definition

*solid section,elset=al, material=aluminum

0.5

```
*solid section,elset=fm, material=foam
0.5
*Nset, nset=loadingnode
310
*nset,nset=symm1
310,59,58,57,56,55,54
*Nset, nset=fix1
360,109,110,111,112,113,4
*elset, elset=symmel
22
*Material, name=aluminum
*Elastic
10000000, 0.35
*Material, name=foam
*Elastic
13100,0.3
*Boundary
symm1, XSYMM
*Boundary
fix1, ENCASTRE
*Step,nlgeom
*Static, riks
```

0.01,0.2,,,,loadingnode,2,-0.7

*Cload

loadingnode, 2, -10.0

*Restart, write, frequency=1

*Output, field, variable=PRESELECT

*Output, history, variable=PRESELECT

*Output, history

*Node Output, nset=fix1

RF2

*Node Output, nset=loadingnode

U2

*Node Output, nset=symm1

RF1

*End Step

VITA

Name: Mahesh Sonawane

Address: 572/21, Yamunanagar, Nigdi, Pune-411044, India

E-mail: mahesh.sonawane@gmail.com

Education: B.E., Mechanical Engineering, Government College of Engineering, Pune, India, 2003.

M.S., Mechanical Engineering, Texas A&M University, 2007